ATLAS recent EFT results

Eleonora Rossi

on behalf of the ATLAS Collaboration

5th General Meeting of the
LHC EFT Working Group
23/05/2022

Latest results

Summary of new results that came out after the 4th LHCEFT General meeting on 23rd May 2022: Talk

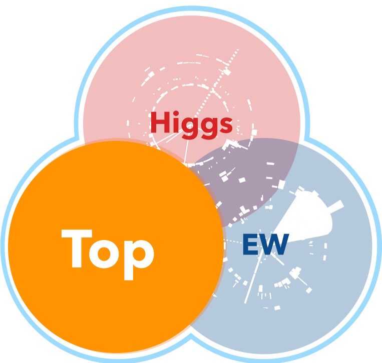

Sketch from Rahul inspired by Ken Mimasu

- $tH(\tau\tau)q$ FCNC: arXiv:2208.11415 (TopFCNC UFO)
- $t\bar{t}$ charge (rapidity) asymmetry: arXiv:2208.12095 (SMEFT@NLO)

Top-quark LHC measurements in the SMEFT

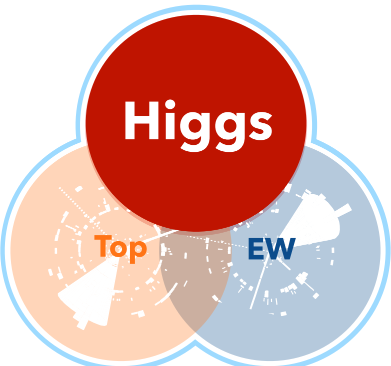

- $H \to \gamma\gamma$: STXS measurements: CERN-EP-2022-094 (SMEFTsim + SMEFT@NLO)

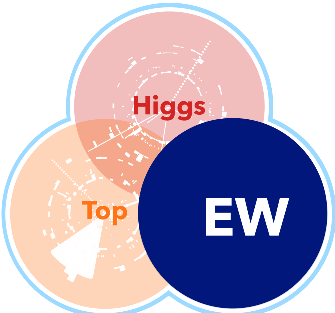

- Electroweak $Z(\nu\bar{\nu})\gamma jj$ production and limits on anomalous quartic gauge couplings: arXiv:2208.12741

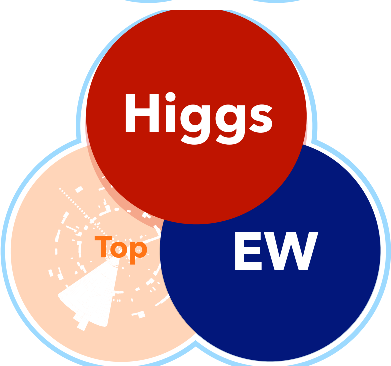

- First ATLAS Global combination (Higgs+EW+EWPO): ATL-PHYS-PUB-2022-037 - (SMEFTsim + SMEFT@NLO)

Focus on results including dim-6 terms and CP-even operators.

EFT: theoretical framework

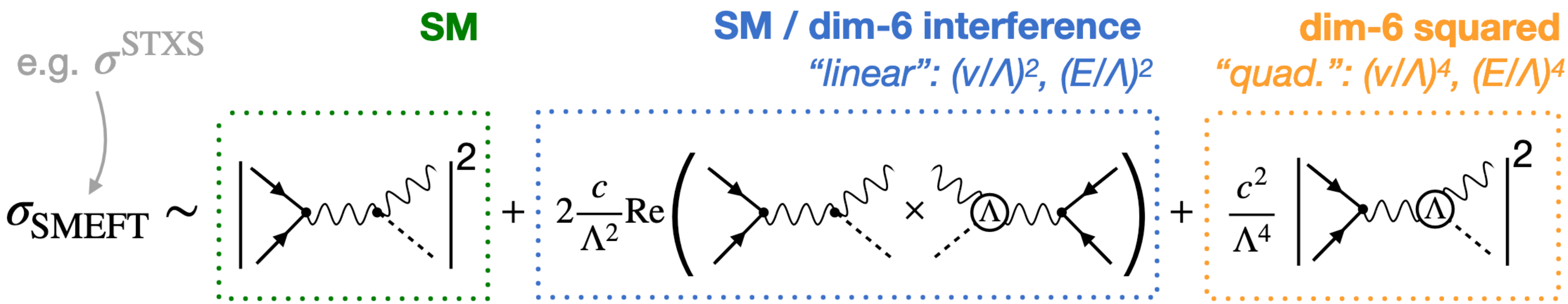

- Warsaw basis, assuming $\Lambda = 1$ TeV.
- SMEFTsim + SMEFT@NLO + TopFCNC.
- Results are usually provided for linear model (+ linear-quadratic models).
- SMEFTsim: different flavour symmetries used to reduce the number of Wilson coefficients.

  ("$U(3)^5$ flavour symmetry","topU3l"): ($H \to \gamma\gamma$, ATLAS Global combination)

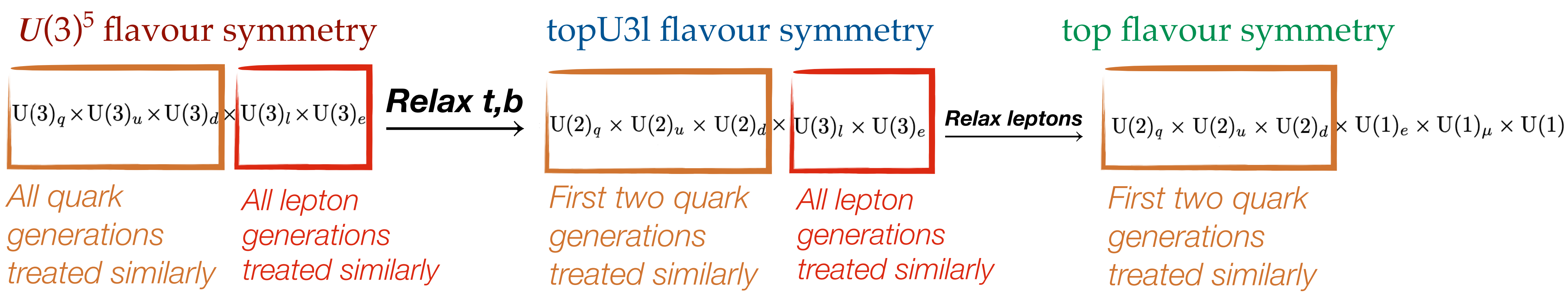

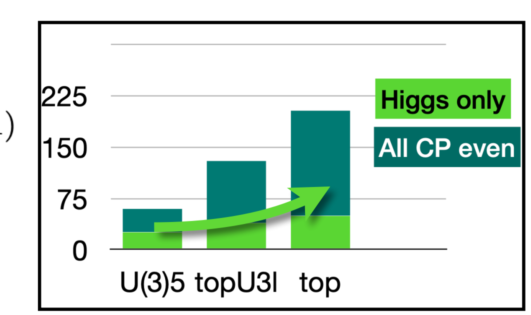

\# of CP-even d=6 operators

Sketch from Andrea Visibile

$tqH(\tau\tau)$ FCNC

arXiv:2208.11415

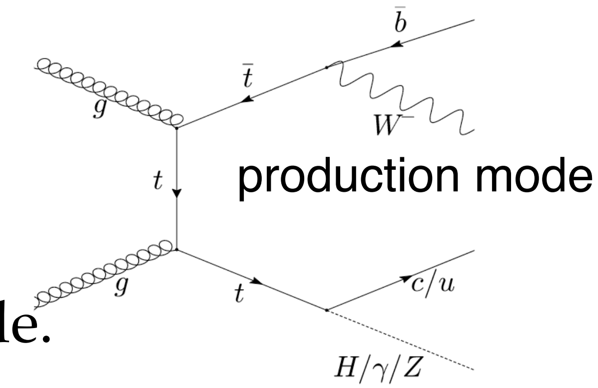

- Search for tqH vertex focusing on $H \to \tau\tau$ in this analysis, where the remaining top decays into a W boson and a b quark - Production & decay mode.
- BDT trained to separate signal and background processes.
- BDT output used in a profile-likelihood fit to extract limits on the FCNC signal processes.
- The FCNC coupling parametrised using dim-6 operators:

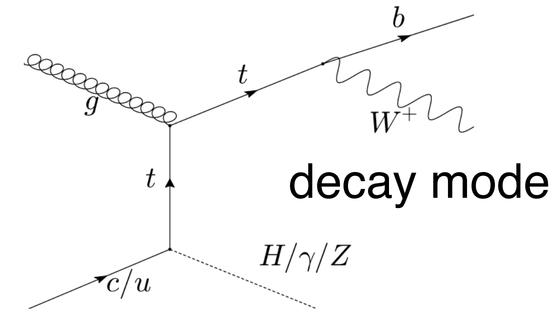

$$\mathcal{L}_{EFT} = \frac{C_{u\phi}^{i3}}{\Lambda^2}(\phi^\dagger\phi)(\bar{q}_i t)\tilde{\phi} + \frac{C_{u\phi}^{3i}}{\Lambda^2}(\phi^\dagger\phi)(\bar{t}_i q)\tilde{\phi}$$

- The coefficient $c_{q\phi}$ can be extracted according to the Madgraph calculation using TopFCNC UFO.
- Improvements of factor 2 in limits on BRs compared to partial Run2 analysis.

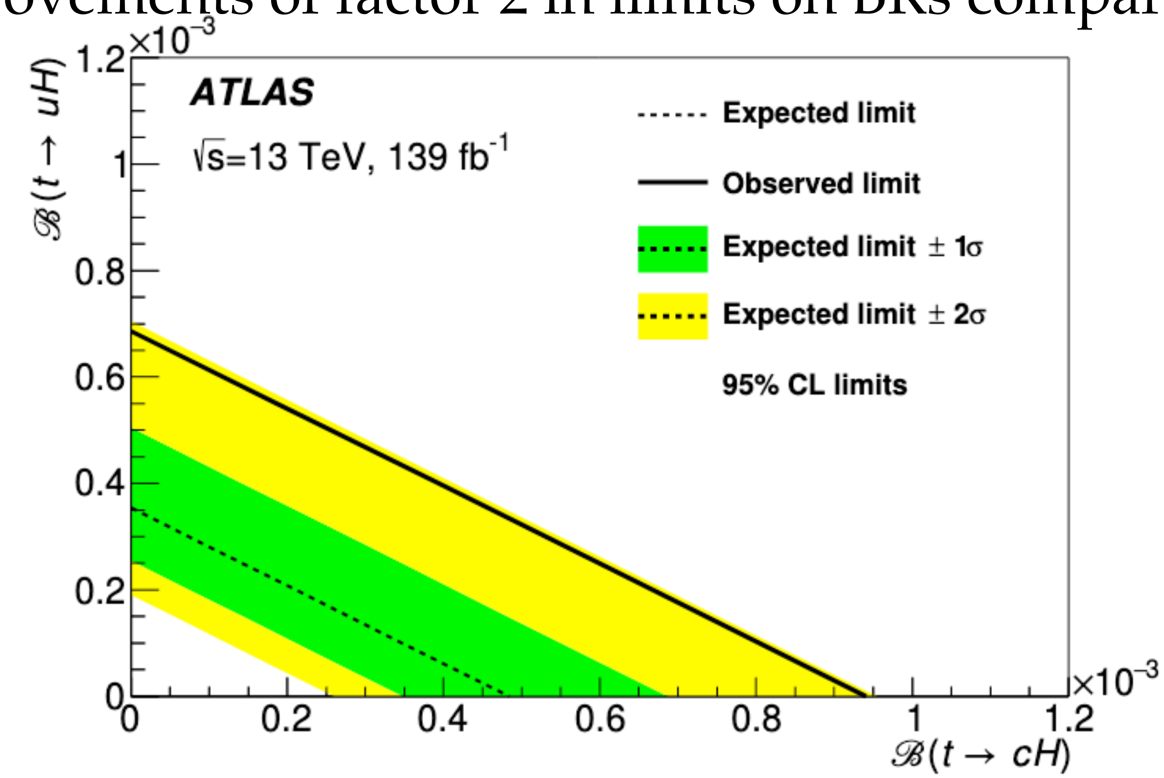

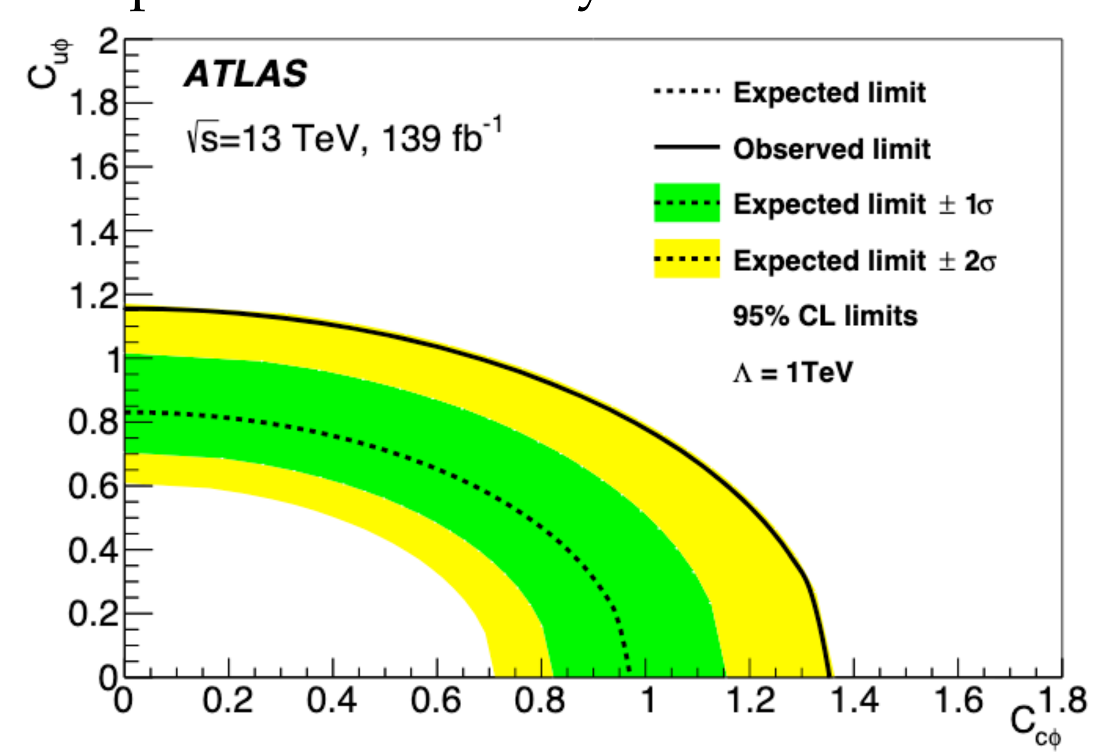

Evidence for the charge asymmetry in $pp \to t\bar{t}$

arXiv:2208.12095

- Inclusive and differential full Run2 measurements of the top–antitop ($t\bar{t}$) charge asymmetry $A_c^{t\bar{t}}$ and the leptonic asymmetry $A_c^{\ell\bar{\ell}}$
- Differential measurements are performed as a function of the invariant mass, transverse momentum and longitudinal boost of the $t\bar{t}$ system.
- Combined results are interpreted in the SMEFT framework.
- **14 four-fermion operators** + 1 operator for top–gluon interaction.

- Large improvement comparing with LHC 8TeV / Tevatron results.
- Interplay between sensitivity, which increases rapidly at higher $m_{t\bar{t}}$, and uncertainty, which grows from 0.2%–0.3% in the lowest mass bin to 2.9% in the highest bin.
- For the linear fit, the tightest limit is obtained in the mass bin from 1 to 1.5 TeV.
- Constraint from the differential $m_{t\bar{t}}$ measurement more than a factor 2 stronger than the one from inclusive measurement (increase in sensitivity with higher $m_{t\bar{t}}$).

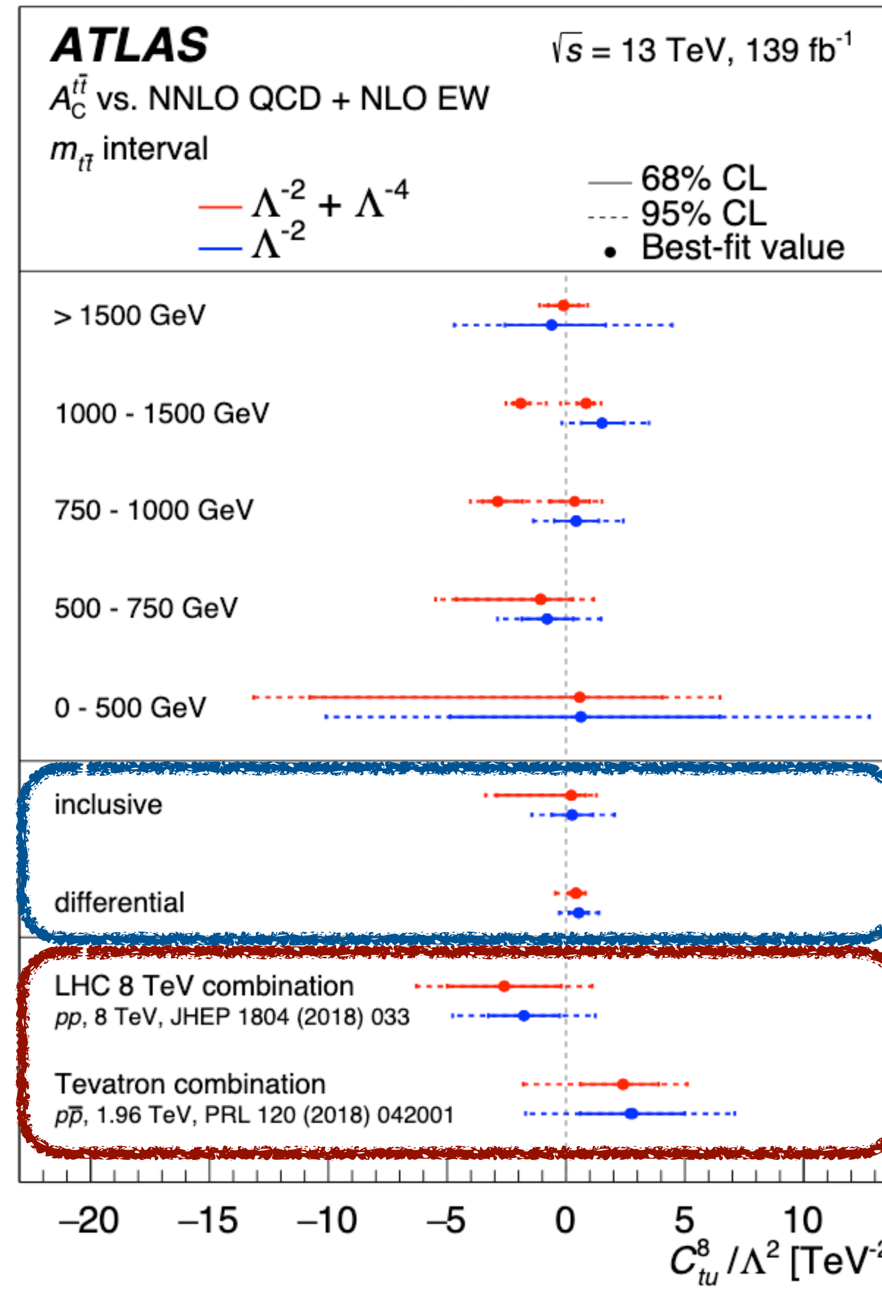

The combined inclusive charge asymmetry is measured to be $A_c^{t\bar{t}}$= 00068 ± 00015, which differs from zero by **4.7 standard deviations.**

Evidence for the charge asymmetry in $pp \to t\bar{t}$

arXiv:2208.12095

- Due to the extra jet in $t\bar{t}j$ production, the QCD structure of the energy asymmetry is not the same as for the charge asymmetry in $t\bar{t}$ production, so the two asymmetries probe different directions in chiral and colour space.
- For colour-octet operators with the same chirality scenarios the shapes of the bounds look very different: the charge asymmetry (dashed / solid red lines) leaves a blind direction which is broken by the energy asymmetry (dashed / solid blue lines) due to operator interference with the QCD amplitude.

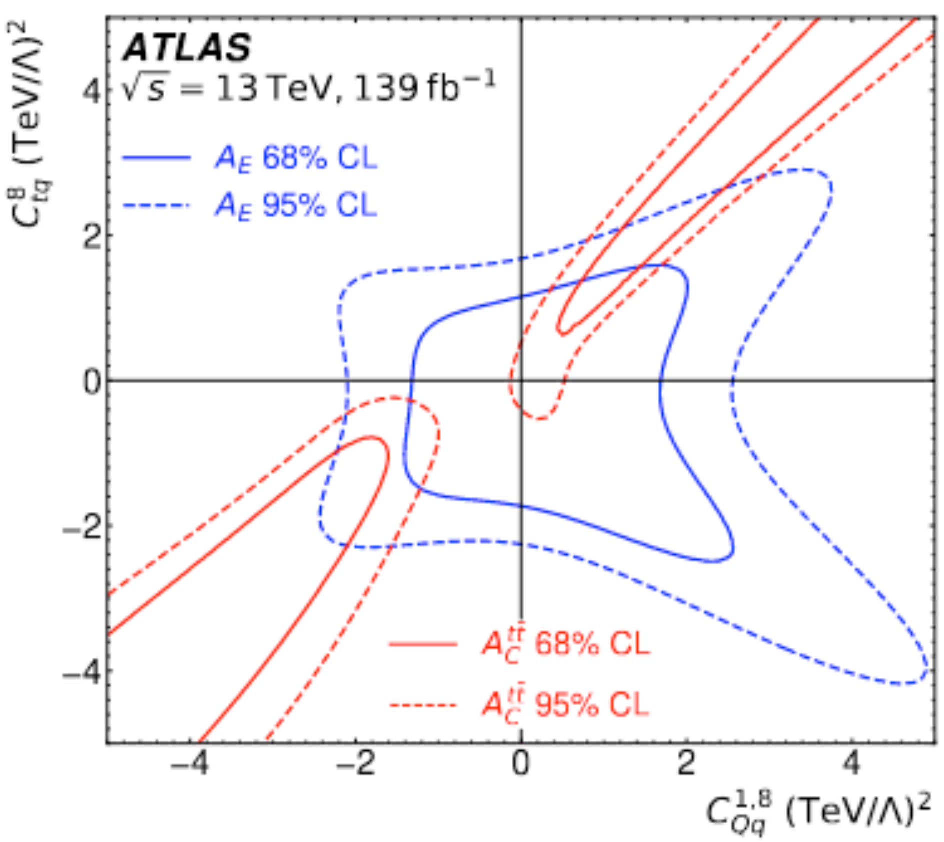

blind direction for rapidity asymmetry broken using energy asymmetry measurement

Bounds on color-octet operators

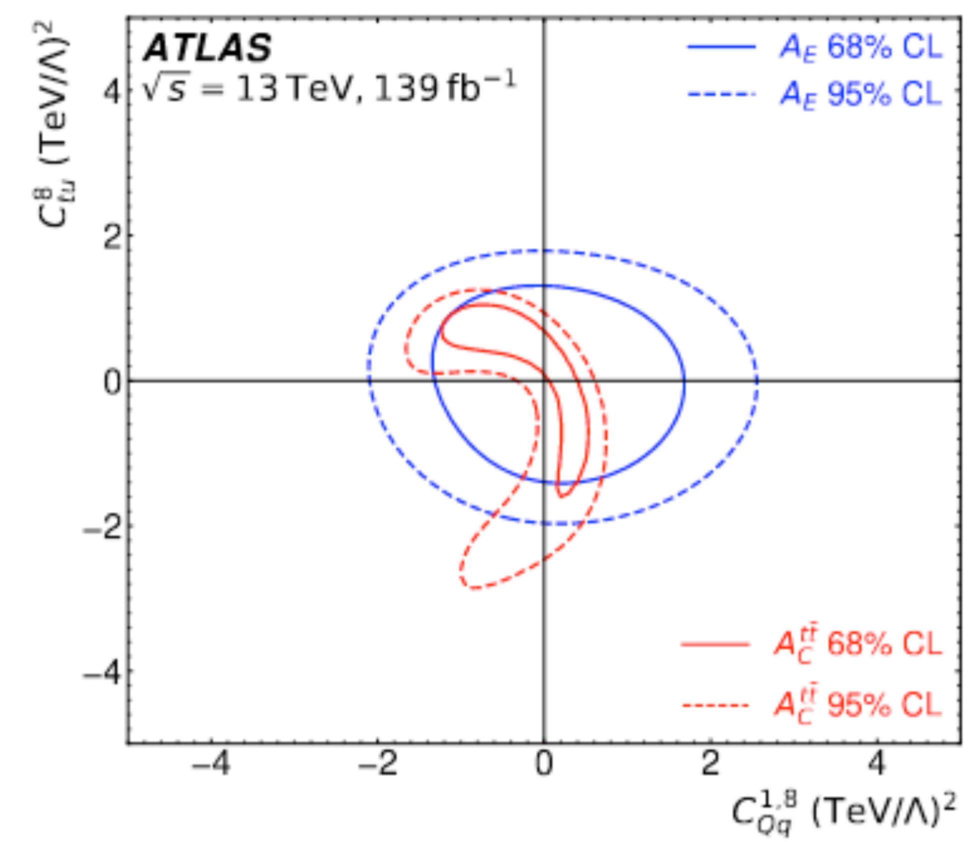

other 2D scans in backup

Higgs + EW: interpretation workflow

STXS x BR
Likelihood/Differential cross-section measurements

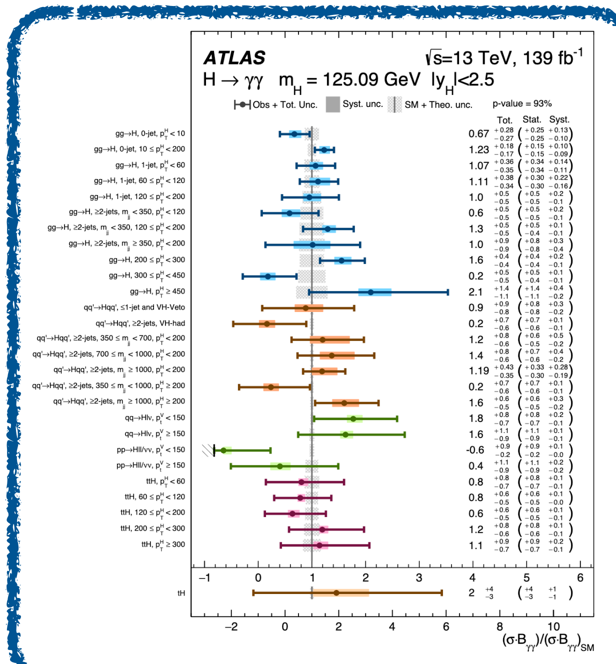

Higgs + EW: interpretation workflow

STXS X BR Likelihood/Differential cross-section measurements → re-parameterisation → EFT Likelihood

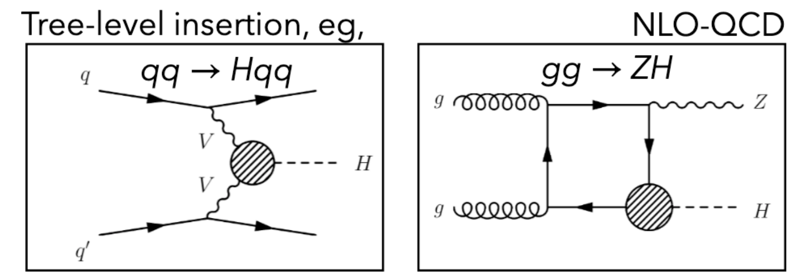

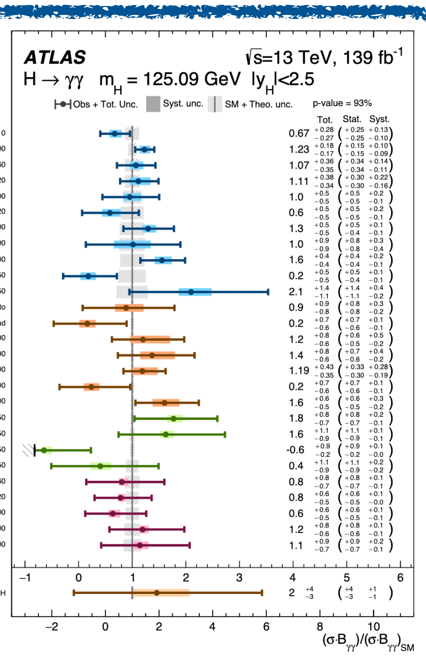

- Dimension-six operator effects are calculated:
  - at tree level using SMEFTsim 3.0.
  - for loop-induced processes (e.g ggH, ggZH): SMEFTatNLO.
  - Analytic formulas for $H \to \gamma\gamma$ including NLO EW corrections and LEP observables.
- Acceptance corrections to account for kinematic differences between SM and SMEFT in Higgs boson decays.
- Effects of width changes of intermediate particles ("propagator corrections") included.

Parameterisation

- Parameterise EFT dependence at the level of STXS and BR, differential cross sections.
- Analytical Expression in term of the Wilson Coefficients.

SMEFTsim v3.0 SMEFT@NLO

Higgs + EW: interpretation workflow

STXS x BR Likelihood/Differential cross-section measurements

re-parameterisation

EFT Likelihood

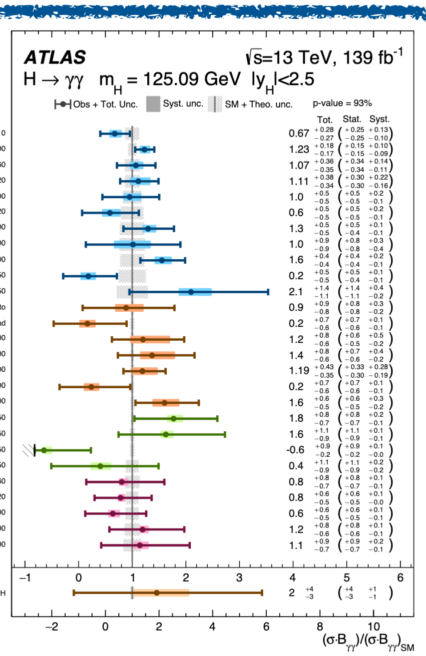

covariance matrix

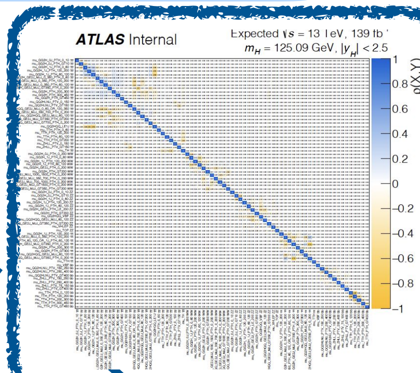

Sensitivity studies

- Removing degenerate directions in the likelihood.
- Keep only the sensitivity directions for final fits.

Parameterisation

- Parameterise EFT dependence at the level of STXS and BR, differential cross sections.
- Analytical Expression in term of the Wilson Coefficients.

SMEFTsim v3.0 SMEFT@NLO

Higgs + EW: interpretation workflow

STXS x BR Likelihood/Differential cross-section measurements

re-parameterisation

EFT Likelihood

sensitive directions

Re-functioned EFT Likelihood

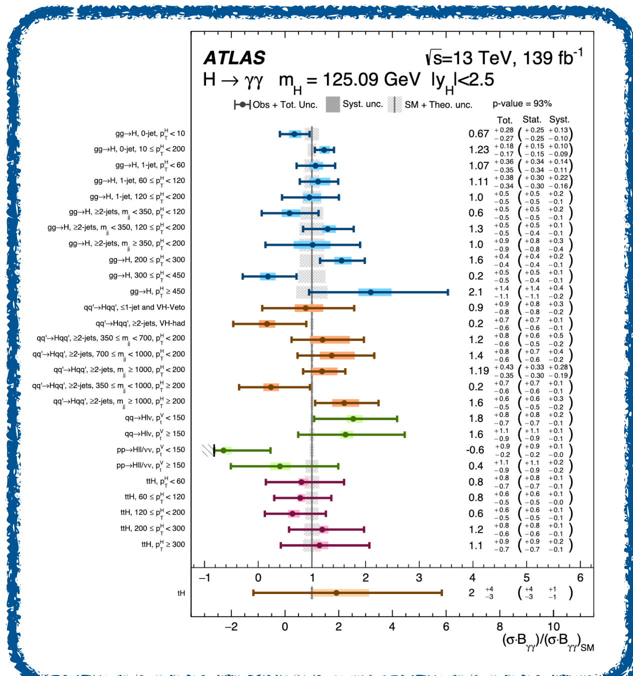

covariance matrix

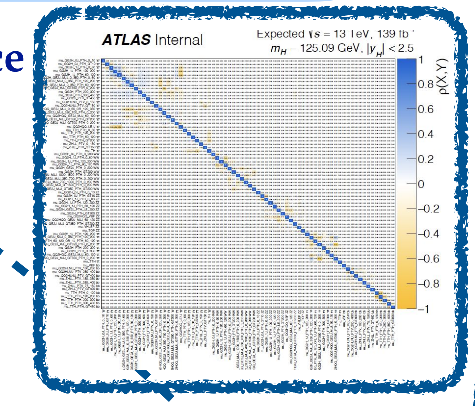

Fit

Sensitivity studies

- Removing degenerate directions in the likelihood.
- Keep only the sensitivity directions for final fits.

Results

Parameterisation

- Parameterise EFT dependence at the level of STXS and BR, differential cross sections.
- Analytical Expression in term of the Wilson Coefficients.

SMEFTsim v3.0

SMEFT@NLO

$H \to \gamma\gamma$: individual WCs constraints

CERN-EP-2022-094

Decay channel	Target Production Modes	$\mathcal{L}$ [fb^{-1}]
$H \to \gamma\gamma$	ggF, VBF, WH, ZH, $t\bar{t}H$, tH	139

- Constraints on individual WCs (one at the time).
- All values compatible with the SM within measurement uncertainties.
- When the sensitivity on one parameter is driven by inclusive event yields, linear and linear+quadratic parameterisations provide similar results.
- Operators with sensitivity to high-p_T^H bins show smaller confidence intervals for the linear+quadratic case.

SMEFTsim: "$U(3)^5$ flavour symmetry"

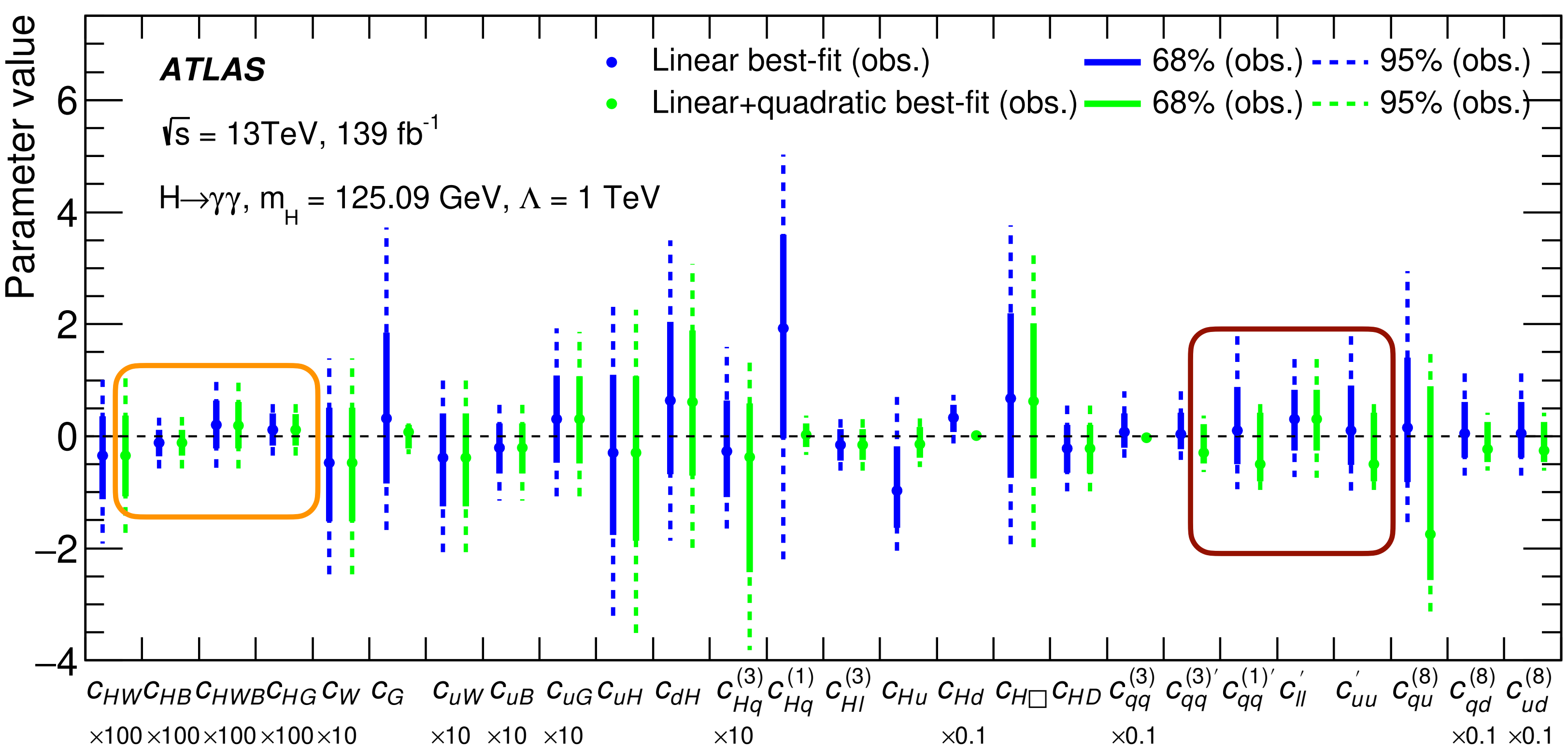

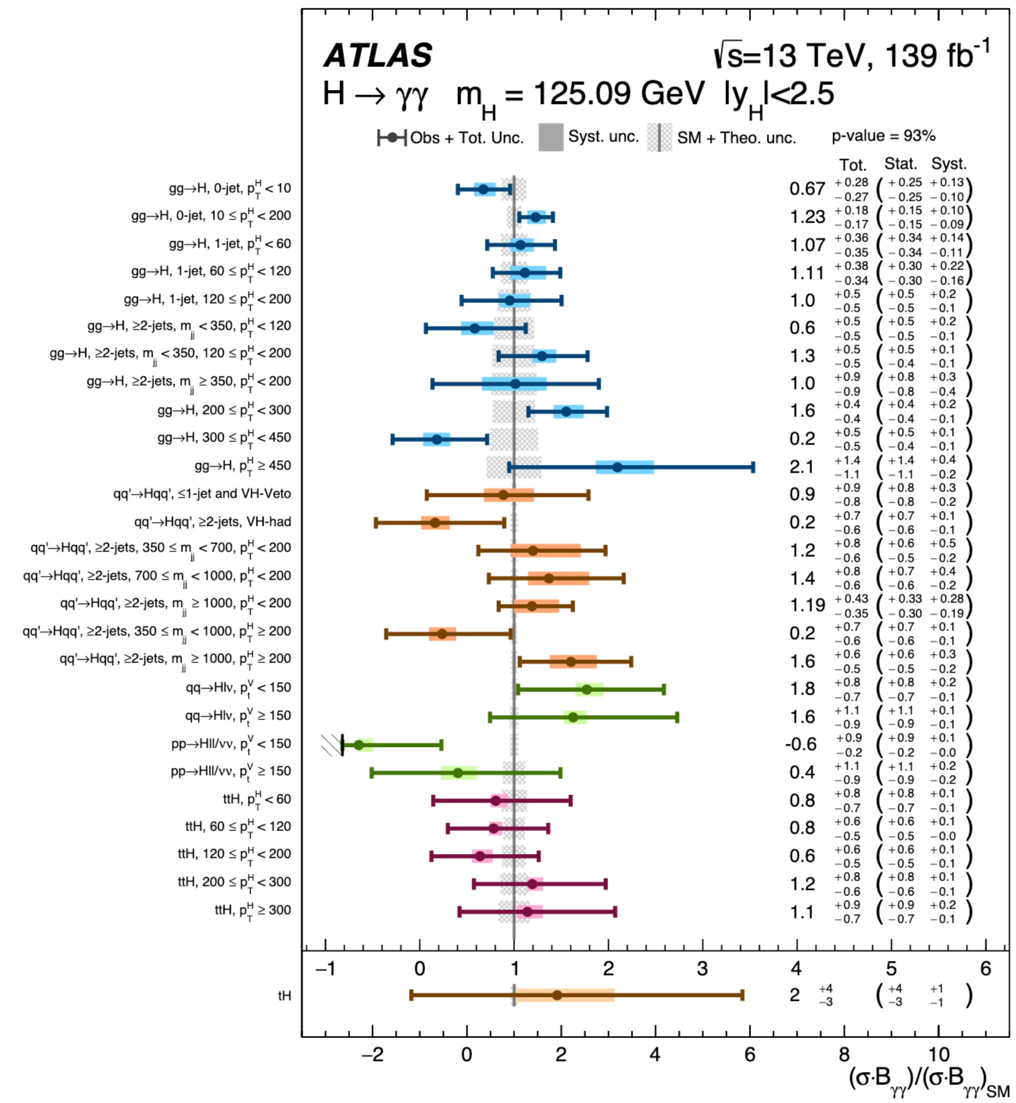

$H \to \gamma\gamma$: constraints on sensitive directions

CERN-EP-2022-094

Decay channel	Target Production Modes	$\mathcal{L}$ [fb^{-1}]
$H \to \gamma\gamma$	ggF, VBF, WH, ZH, $t\bar{t}H$, tH	139

- Cannot constraints simultaneously all the WCs the STXS measurements are affected by (34).
- Operators grouped according to the eigenvectors of the information matrix of the measurement.
- Inclusion of propagator corrections has been tested.
- Both linear and linear+quadratic results are provided.
- All results are in agreement with SM expectations.

12 directions

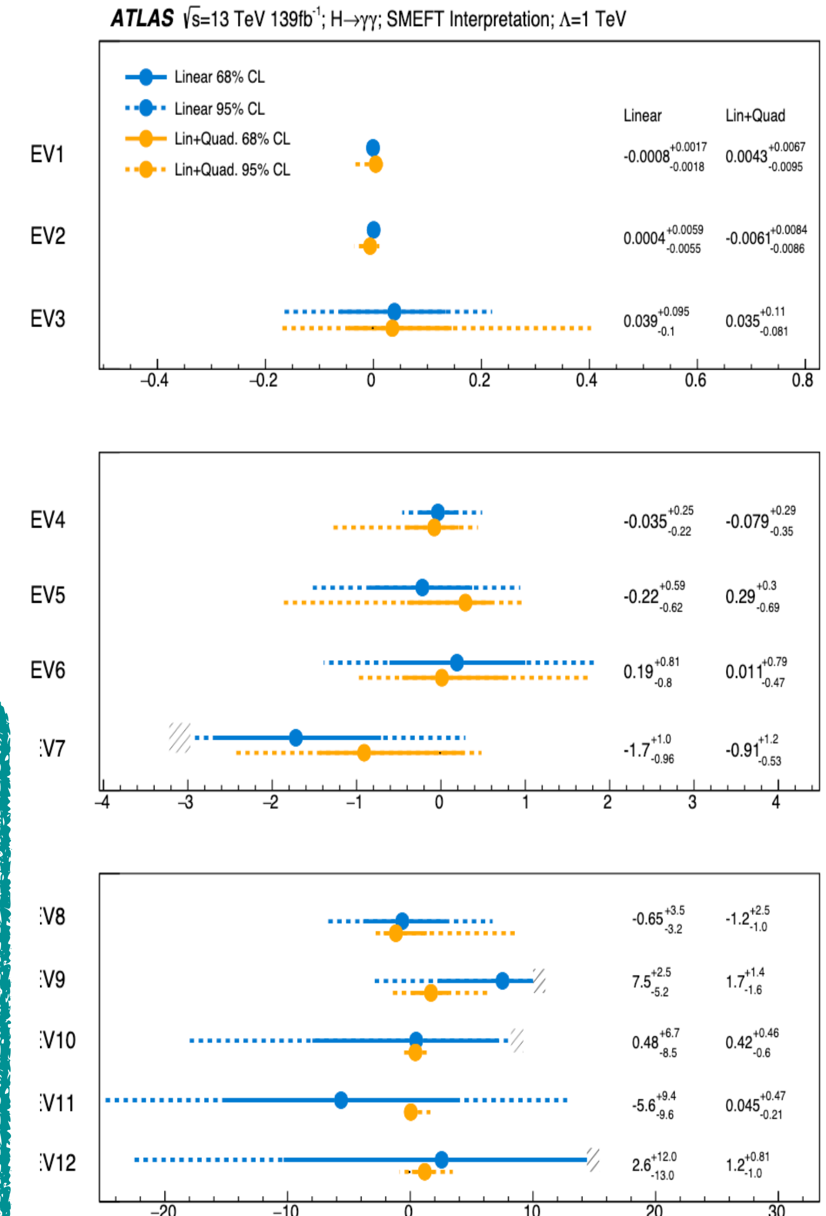

10 directions from Higgs 2020 combination (3 channels)

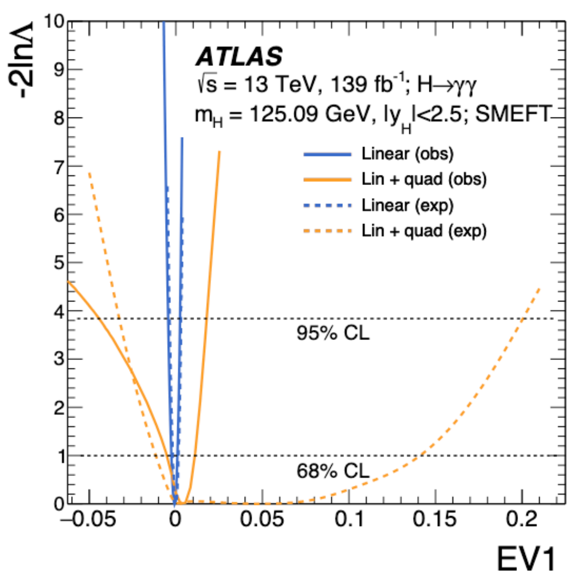

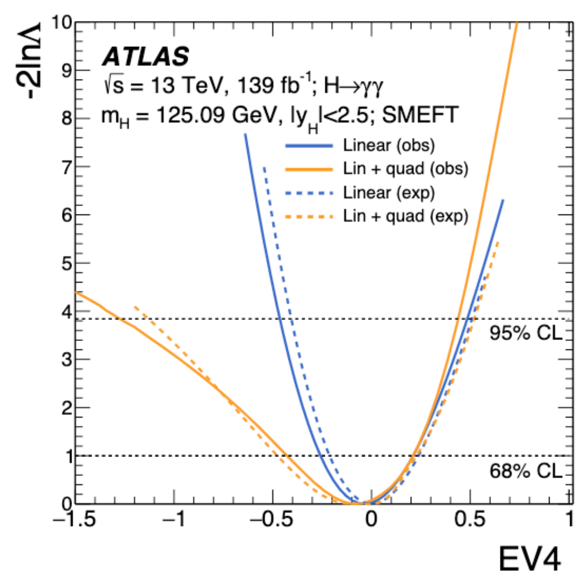

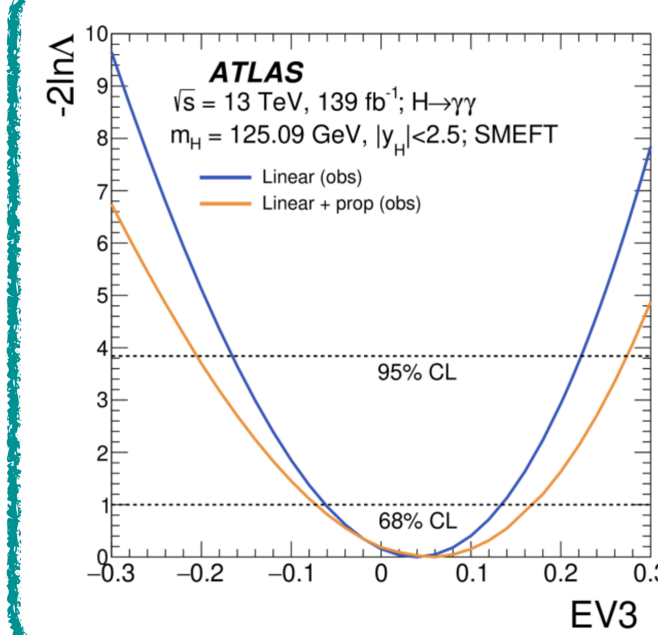

First ATLAS Global combination

Decay channel	Target Production Modes	$\mathcal{L}$ [fb^{-1}]
$H \to \gamma\gamma$	ggF, VBF, $WH, ZH, t\bar{t}H, tH$	139
$H \to ZZ^*$	ggF, VBF, $WH, ZH, t\bar{t}H(4\ell)$	139
$H \to WW^*$	ggF, VBF	139
$H \to \tau\tau$	ggF, VBF, $WH, ZH, t\bar{t}H(\tau_{\text{had}}\tau_{\text{had}})$	139
	WH, ZH	139
$H \to b\bar{b}$	VBF	126
	$t\bar{t}H$	139

- ATLAS Higgs boson data (2021 combination)
- Higgs boson production and decay combined measurements in STXS bins

Higgs Combination

WW,WZ,4l, Z+2jets combination

Process	Important phase space requirements	Observable	$\mathcal{L}$ [fb^{-1}]
$pp \to e^{\pm}\nu\mu^{\mp}\nu$	$m_{\ell\ell} > 55$ GeV, $p_T^{\text{jet}} < 35$ GeV	$p_T^{\text{lead. lep.}}$	36
$pp \to \ell^{\pm}\nu\ell^{+}\ell^{-}$	$m_{\ell\ell} \in (81, 101)$ GeV	m_T^{WZ}	36
$pp \to \ell^{+}\ell^{-}\ell^{+}\ell^{-}$	$m_{4\ell} > 180$ GeV	m_{Z2}	139
$pp \to \ell^{+}\ell^{-}jj$	$m_{jj} > 1000$ GeV, $m_{\ell\ell} \in (81, 101)$ GeV	$\Delta\phi_{jj}$	139

- ATLAS electroweak data
- Differential cross-section measurements for diboson and Z production via VBF

Observable	Measurement	Prediction	Ratio
Γ_Z [MeV]	2495.2 ± 2.3	2495.7 ± 1	0.9998 ± 0.0010
R^0_ℓ	20.767 ± 0.025	20.758 ± 0.008	1.0004 ± 0.0013
R^0_c	0.1721 ± 0.0030	0.17223 ± 0.00003	0.999 ± 0.017
R^0_b	0.21629 ± 0.00066	0.21586 ± 0.00003	1.0020 ± 0.0031
$A^{0,\ell}_{\text{FB}}$	0.0171 ± 0.0010	0.01718 ± 0.00037	0.995 ± 0.062
$A^{0,c}_{\text{FB}}$	0.0707 ± 0.0035	0.0758 ± 0.0012	0.932 ± 0.048
$A^{0,b}_{\text{FB}}$	0.0992 ± 0.0016	0.1062 ± 0.0016	0.935 ± 0.021
σ^0_{had} [pb]	41488 ± 6	41489 ± 5	0.99998 ± 0.00019

Precision Electroweak Measurements on the Z Resonance

- Electroweak precision observables measured at LEP and SLC
- Eight pseudo observables describing the physics at the Z-pole are interpreted.
- Measurement probed with high sensitivity O(1 - 0.01 %)

First ATLAS Global combination

Higgs Combination

Decay channel	Target Production Modes	$\mathcal{L}$ [fb^{-1}]
$H \to \gamma\gamma$	ggF, VBF, $WH, ZH, t\bar{t}H, tH$	139
$H \to ZZ^*$	ggF, VBF, $WH, ZH, t\bar{t}H(4\ell)$	139
$H \to WW^*$	ggF, VBF	139
$H \to \tau\tau$	ggF, VBF, $WH, ZH, t\bar{t}H(\tau_{\text{had}}\tau_{\text{had}})$	139
	WH, ZH	139
$H \to b\bar{b}$	VBF	126
	$t\bar{t}H$	139

- ATLAS Higgs boson data (2021 combination)
- Higgs boson production and decay combined measurements in STXS bins

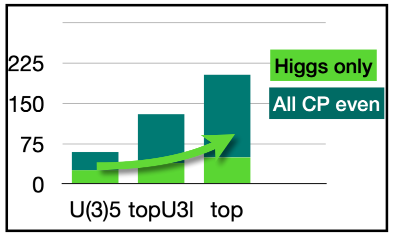

\# of CP-even d=6 operators

SMEFTsim: “topU3l” flavour symmetry”

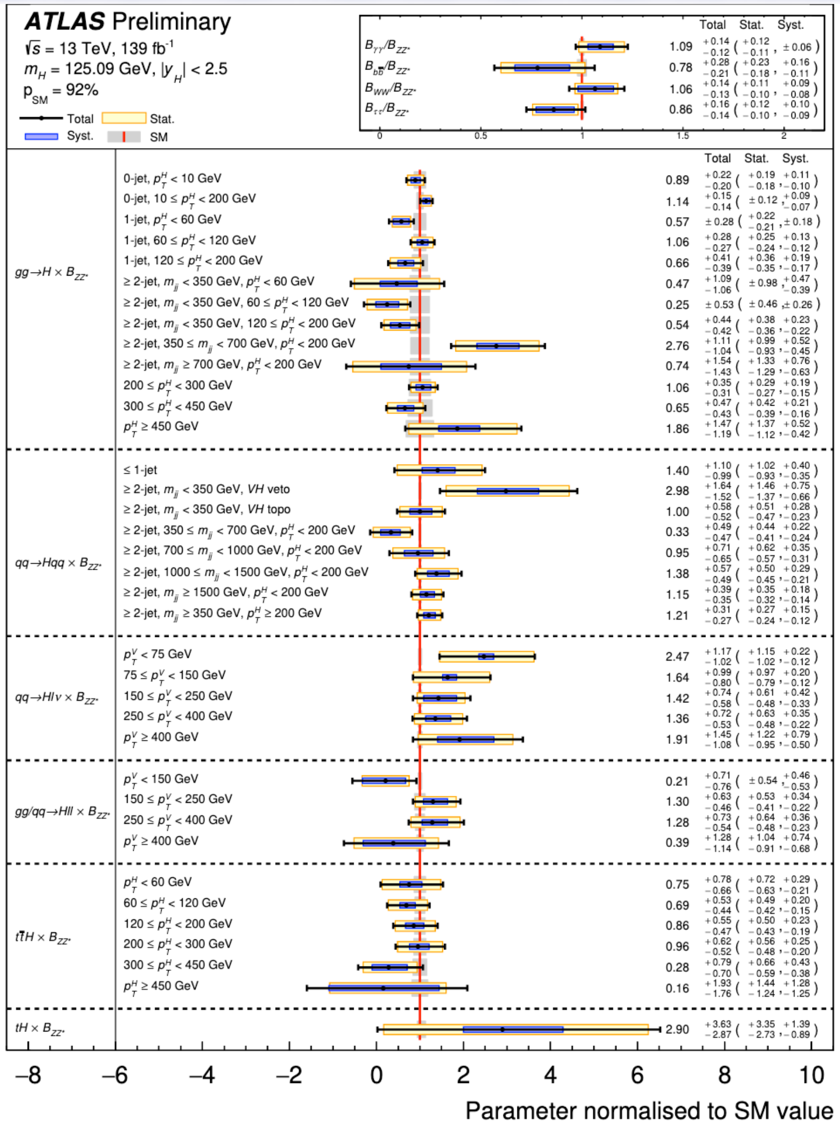

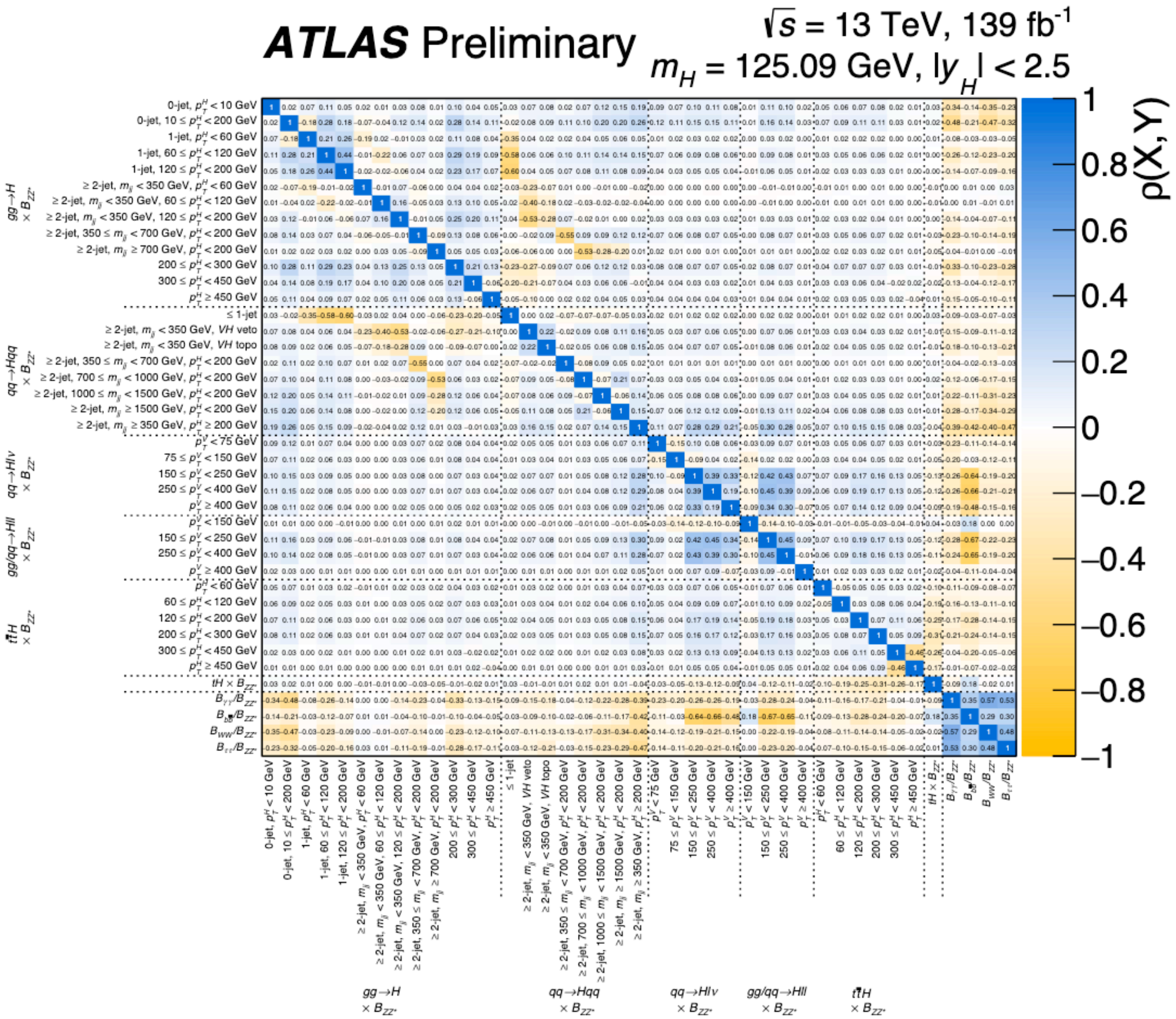

First ATLAS Global combination

WW,WZ,4l, Z+2jets combination

$$L(\boldsymbol{x}|\boldsymbol{c},\boldsymbol{\theta}) = \frac{1}{\sqrt{(2\pi)^{n_{\text{bins}}}\det(V)}} \exp\left(-\frac{1}{2}\Delta\boldsymbol{x}^{\top}(\boldsymbol{c},\boldsymbol{\theta})\,V^{-1}\Delta\boldsymbol{x}(\boldsymbol{c},\boldsymbol{\theta})\right) \times \prod_{i}^{n_{\text{theo syst}}} f_i(\theta_{\text{theo syst},i}) \times \prod_{i}^{n_{\text{exp syst}}} f_i(\theta_{\text{exp syst},i})\,.$$

Multivariate gaussian

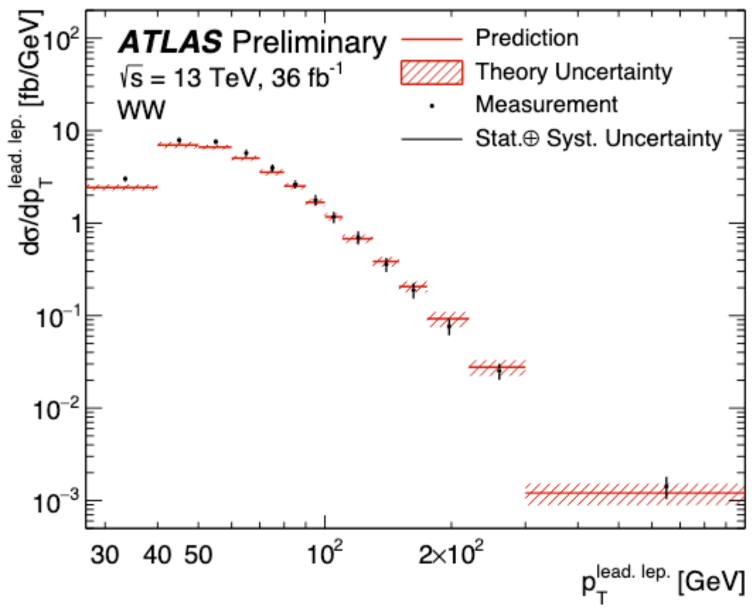

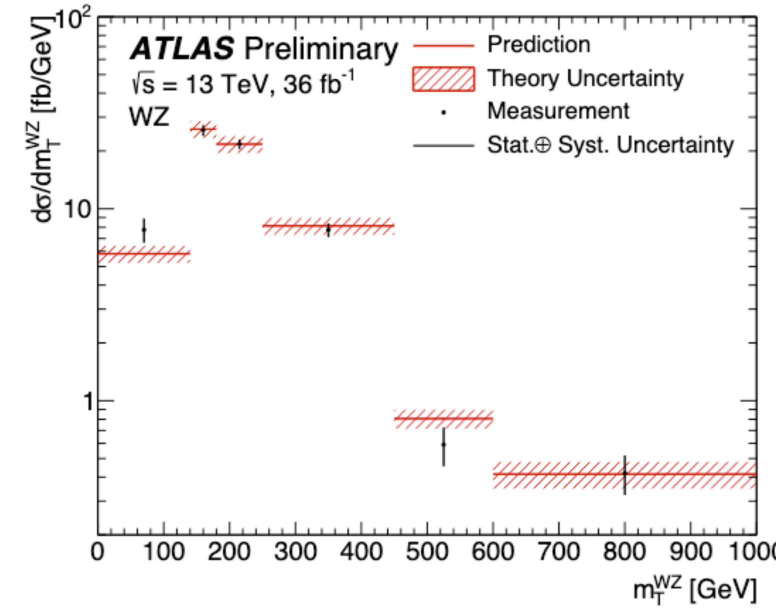

Process	Important phase space requirements	Observable	$\mathcal{L}$ [fb^{-1}]
$pp \to e^{\pm}\nu\mu^{\mp}\nu$	$m_{\ell\ell} > 55$ GeV, $p_{\mathrm{T}}^{\mathrm{jet}} < 35$ GeV	$p_{\mathrm{T}}^{\text{lead. lep.}}$	36
$pp \to \ell^{\pm}\nu\ell^{+}\ell^{-}$	$m_{\ell\ell} \in (81, 101)$ GeV	m_{T}^{WZ}	36
$pp \to \ell^{+}\ell^{-}\ell^{+}\ell^{-}$	$m_{4\ell} > 180$ GeV	m_{Z2}	139
$pp \to \ell^{+}\ell^{-}jj$	$m_{jj} > 1000$ GeV, $m_{\ell\ell} \in (81, 101)$ GeV	$\Delta\phi_{jj}$	139

- ATLAS electroweak data
- Differential cross-section measurements for diboson and Z production via VBF

SMEFTsim: "topU3l" flavour symmetry"

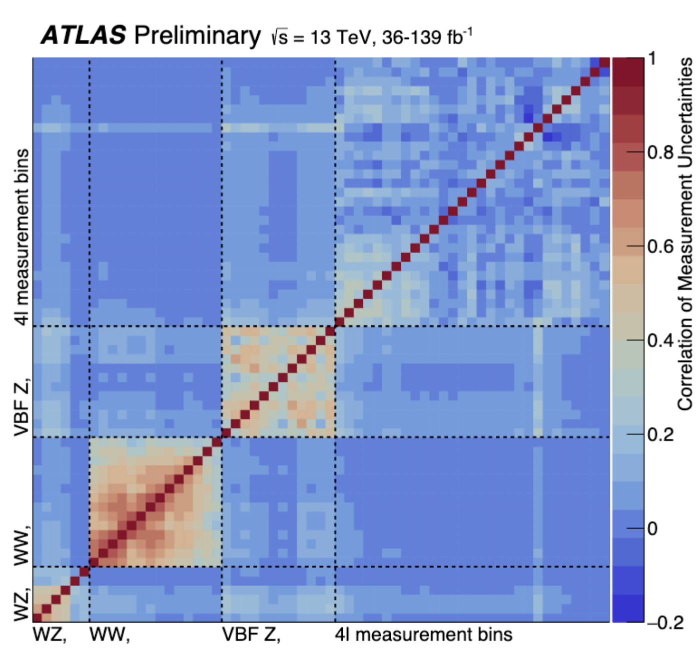

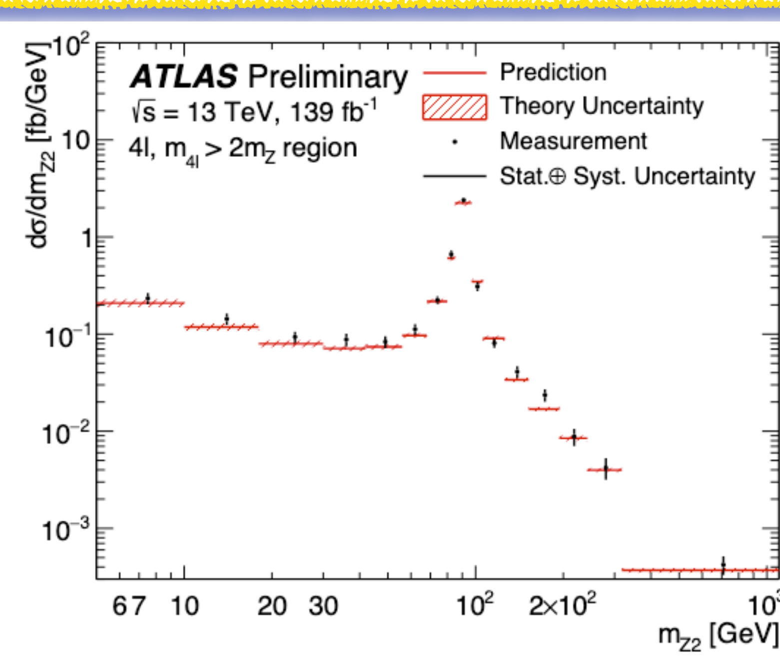

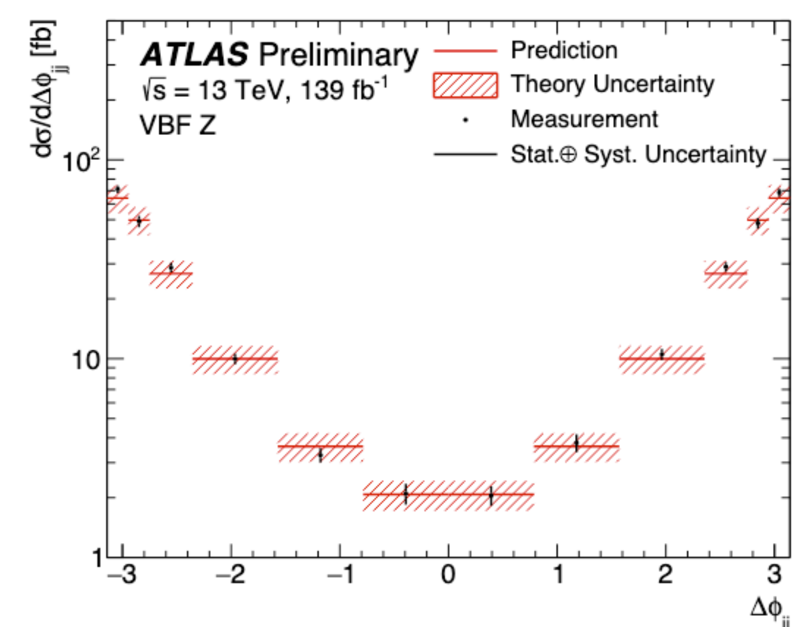

First ATLAS Global combination

Precision Electroweak Measurements on the Z Resonance

$\Gamma_Z, R_\ell^0, R_c^0, R_b^0, A_{FB}^{0,\ell}, A_{FB}^{0,c}, A_{FB}^{0,b}, \sigma_{had}^0$

- R_ℓ^0, R_c^0, R_b^0: **Ratio of partial decay widths**
- $A_{FB}^{0,\ell}, A_{FB}^{0,c}, A_{FB}^{0,b}$: **Forward-backward asymmetry**
- σ_{had}^0: **Hadronic pole cross section**

- Tight limit provided by LEP-> only sensitive to a limited number of parameters.
- Parametrisation of EW pole observables only in the linear approximations:
  - Two different fit setups: Higgs+EW and Higgs+EW+EWPO
- The likelihood is modelled as a multivariate Gaussian, both theoretical and experimental uncertainties are included in the covariance matrix.

EWPD in the SMEFT to dimension eight

Observable	Measurement	Prediction	Ratio
Γ_Z [MeV]	2495.2 ± 2.3	2495.7 ± 1	0.9998 ± 0.0010
R_ℓ^0	20.767 ± 0.025	20.758 ± 0.008	1.0004 ± 0.0013
R_c^0	0.1721 ± 0.0030	0.17223 ± 0.00003	0.999 ± 0.017
R_b^0	0.21629 ± 0.00066	0.21586 ± 0.00003	1.0020 ± 0.0031
$A_{FB}^{0,\ell}$	0.0171 ± 0.0010	0.01718 ± 0.00037	0.995 ± 0.062
$A_{FB}^{0,c}$	0.0707 ± 0.0035	0.0758 ± 0.0012	0.932 ± 0.048
$A_{FB}^{0,b}$	0.0992 ± 0.0016	0.1062 ± 0.0016	0.935 ± 0.021
σ_{had}^0 [pb]	41488 ± 6	41489 ± 5	0.99998 ± 0.00019

- **Electroweak precision observables measured at LEP and SLC**
- Eight pseudo observables describing the physics at the Z-pole are interpreted.
- Measurement probed with high sensitivity O(1 - 0.01 %)

ATLAS Global combination: one at a time

ATL-PHYS-PUB-2022-037

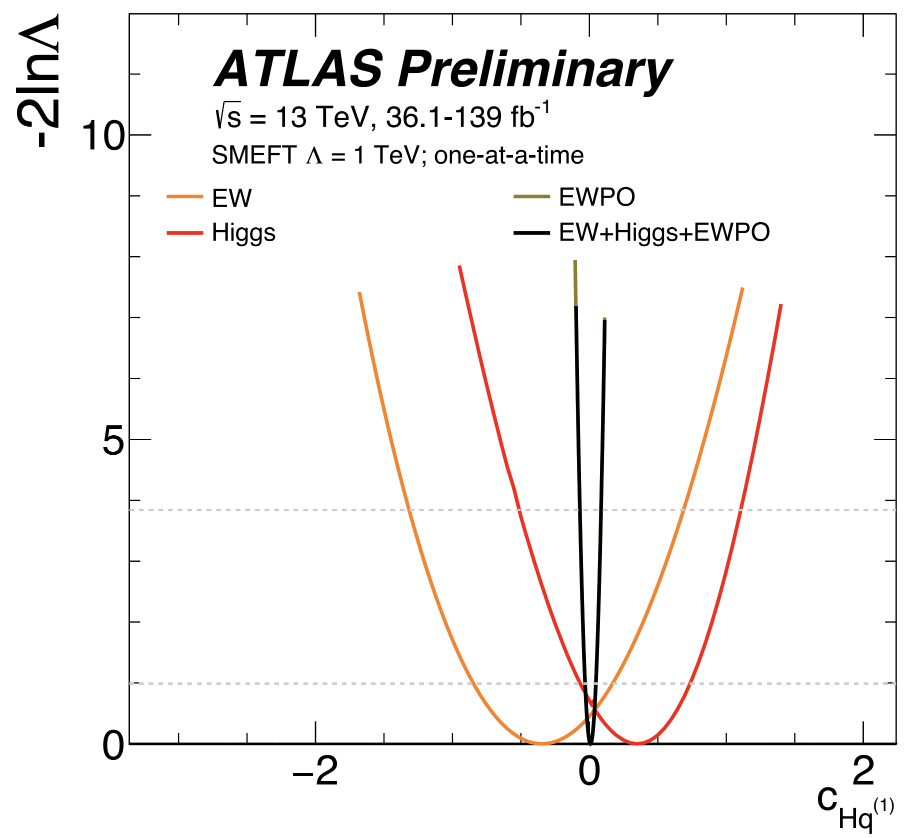

- One parameter at a time scans to compare sensitivity to an operator across the 3 measurement groups;
    - all remaining Wilson coefficients fixed to zero;
    - correlations between operators are neglected.

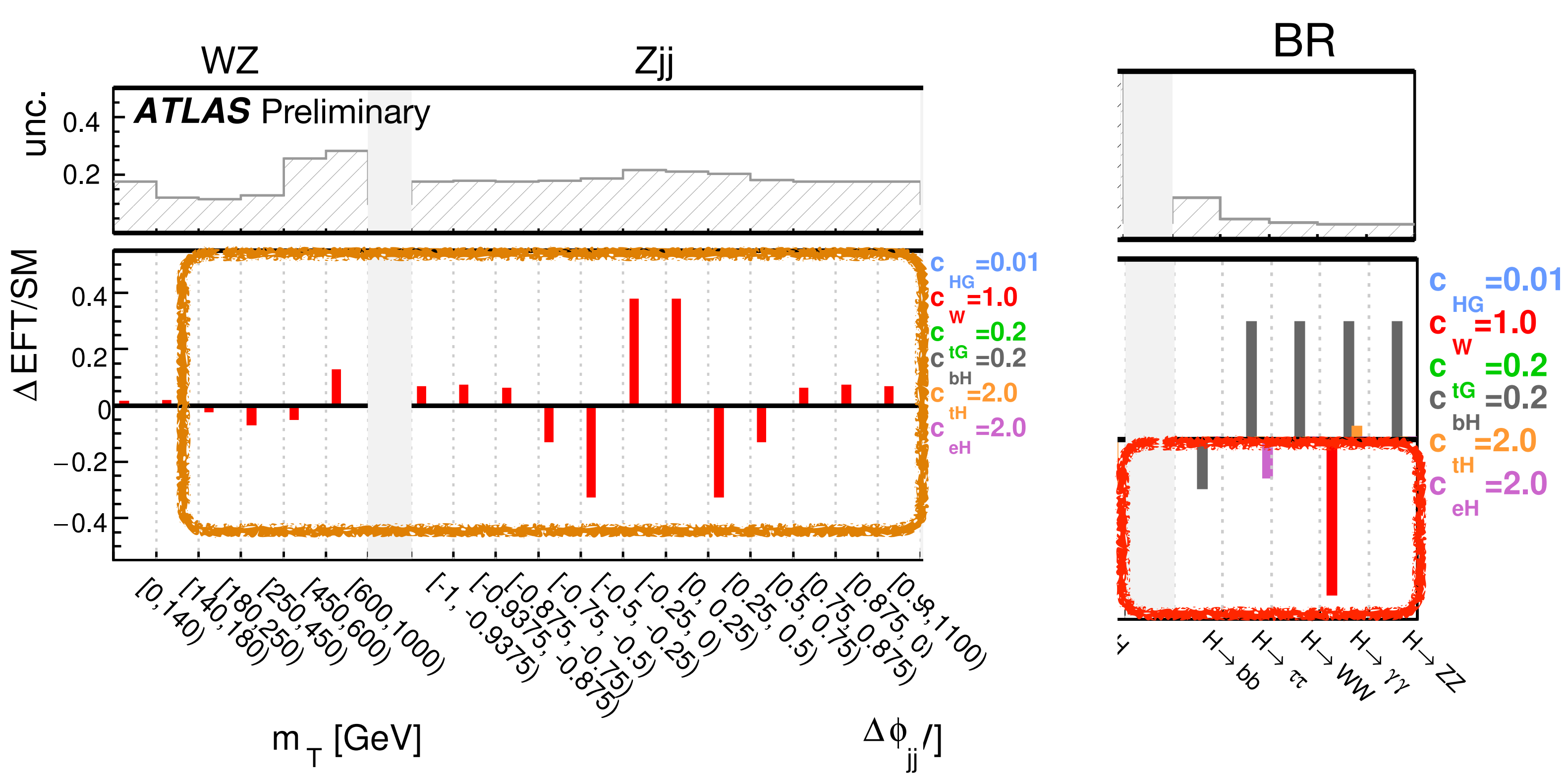

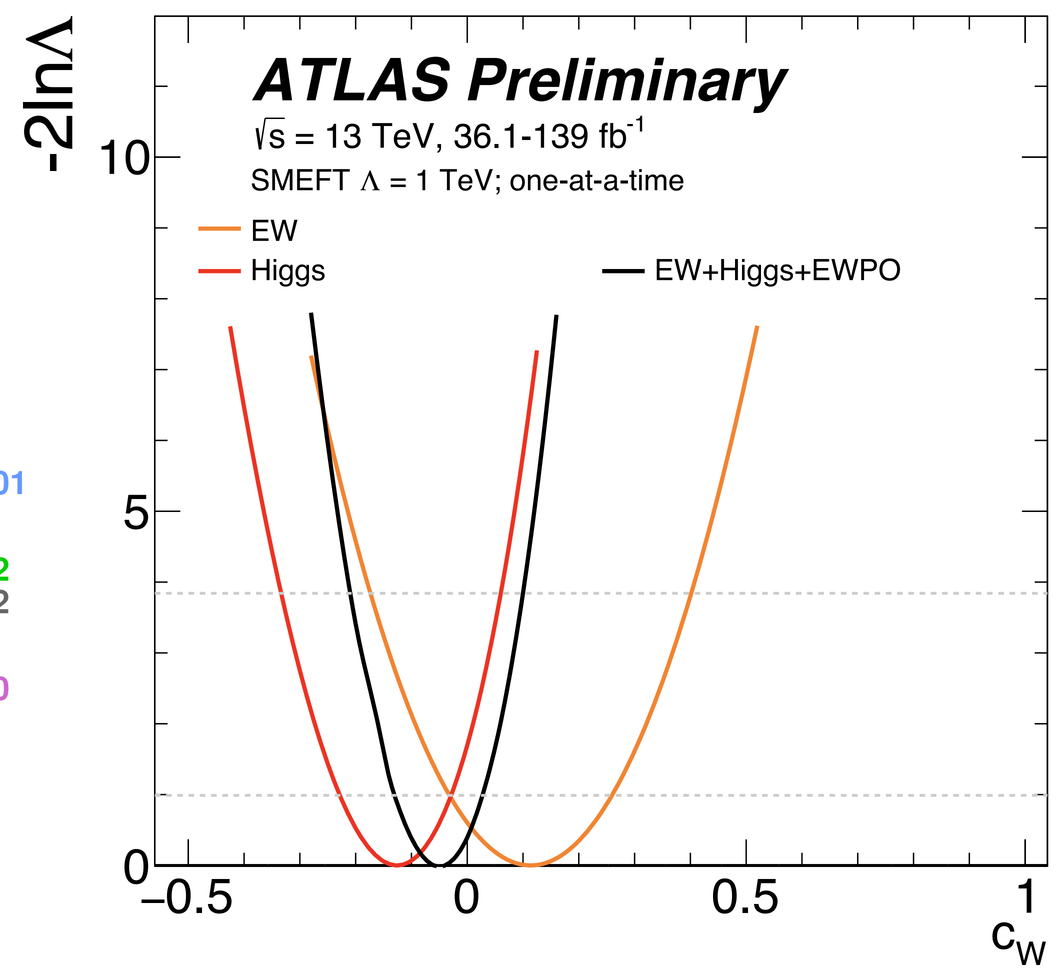

ATLAS Global combination

HIGGS+EW

- Constraining **7** individual and **17** linear combinations of Wilson coefficients.
- Data overlap across datasets checked -> remove from the combination whenever relevant.

- PCA to identify sensitive directions-> a modified basis of linear combinations of WCs is defined.
- The fit uses sensitivity eigenvectors instead of original WCs.

Most stringent constraints

Constrained by both diboson and VH measurements

Weakly constrained fit directions-> quadratic contributions are often large; validity of the obtained constraints is questionable

ATL-PHYS-PUB-2022-037

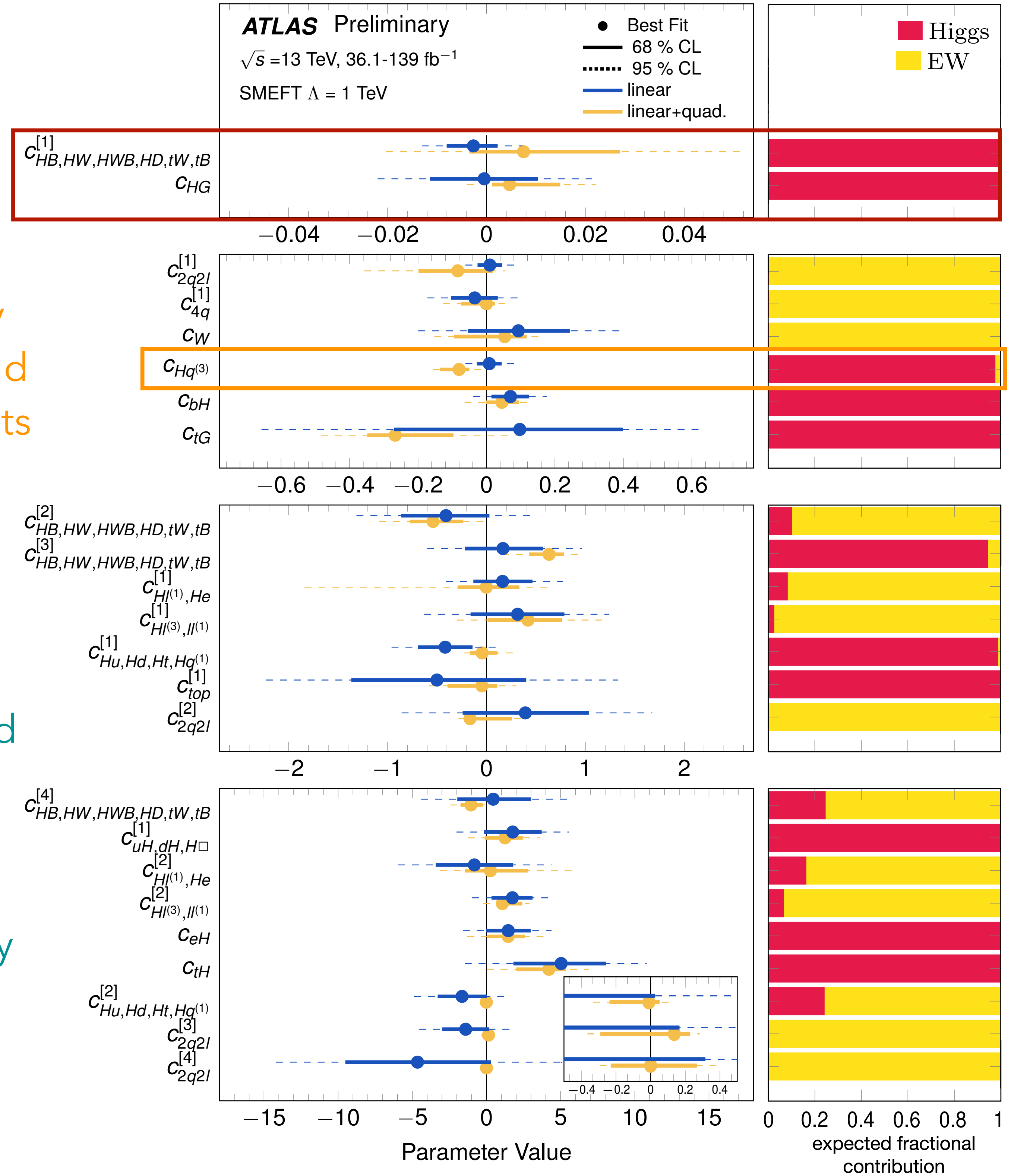

ATLAS Global combination

HIGGS+EW+EWPO

- Constraining **6** individual and **22** linear combinations of Wilson coefficients.
- Several constraints driven by both ATLAS and LEP/SLD.
- Complementary information.
- Linear fits agree with the SM expectation for most fitted parameters, except for:
  - $c^{[4]}_{HVV,Vff}$ → excess driven by a well-known discrepancy in $A^{0,b}_{FB}$ from the SM expectation.

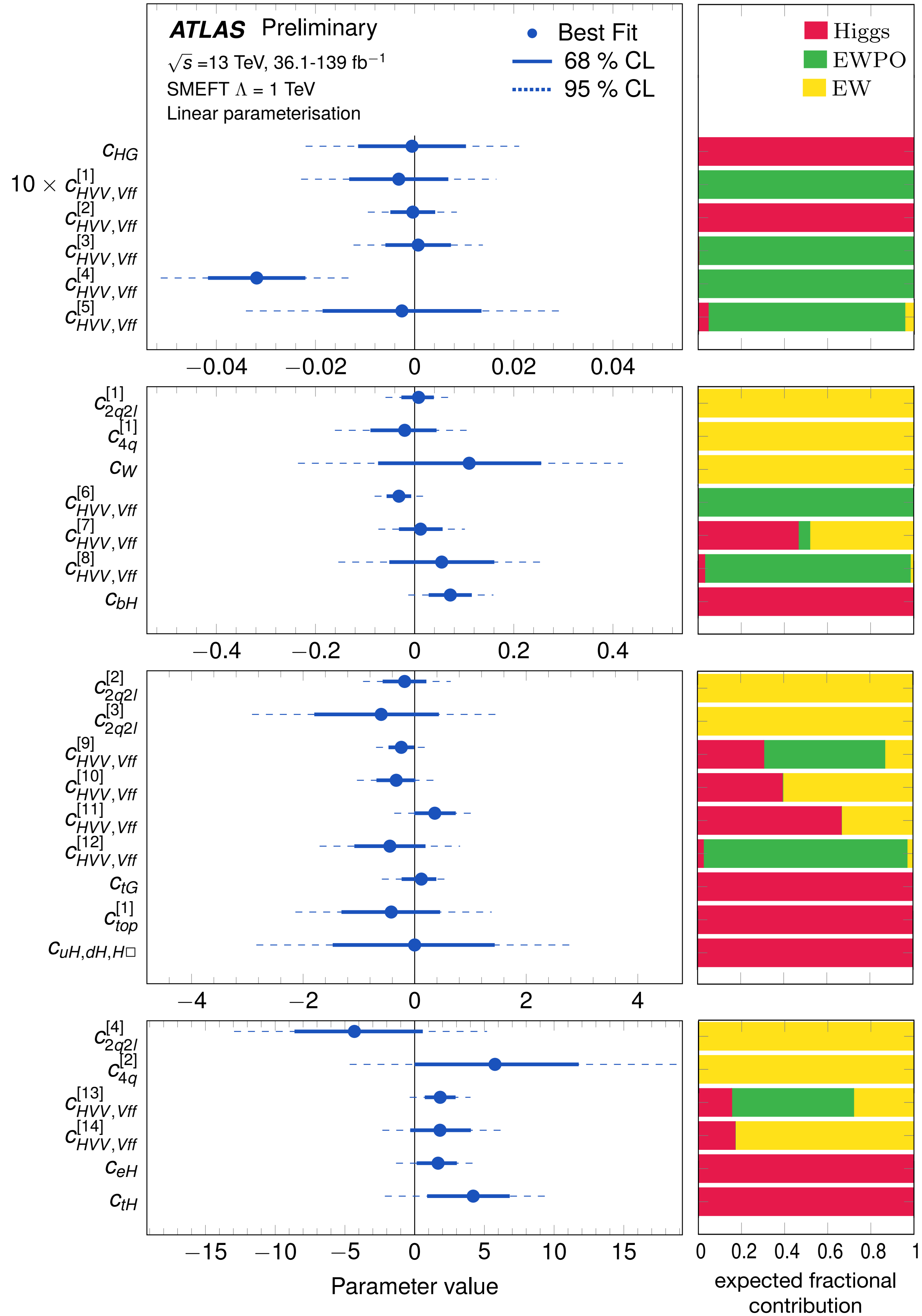

ATL-PHYS-PUB-2022-037

ATLAS Global combination: simplified likelihood

ATL-PHYS-PUB-2022-037

- Simplified likelihood model:
  - format to deliver results for re-interpretation;
  - signal strength modifier + correlation matrix.
- Results from the full likelihood fit compared to those using a simplified likelihood following a multi-variate Gaussian approach:
  - minimal differences between the two methods;
  - the simplified model is nuisance parameter free, as the effect of all uncertainties is encoded in the covariance matrix-> computationally inexpensive.
- Signal strength modifiers + correlation matrix available, preparing shared parameterisation.

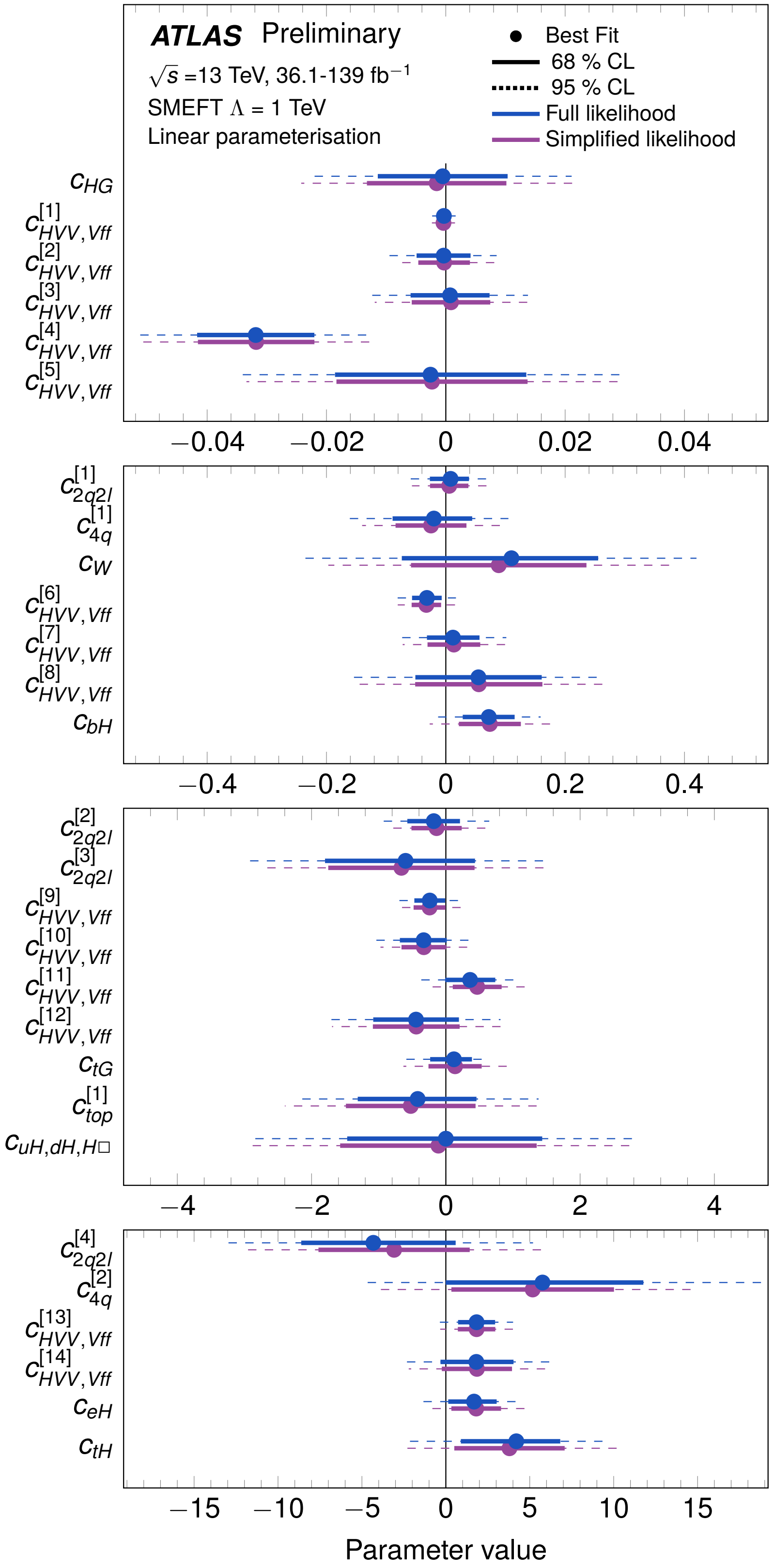

What's next

- First global ATLAS EFT interpretation available, also providing a simplified likelihood model for re-interpretation.
    - Well established framework used to perform the ATLAS Global combination.
    - Combination with additional Top + EW analyses ongoing-> provide complementary sensitivity.

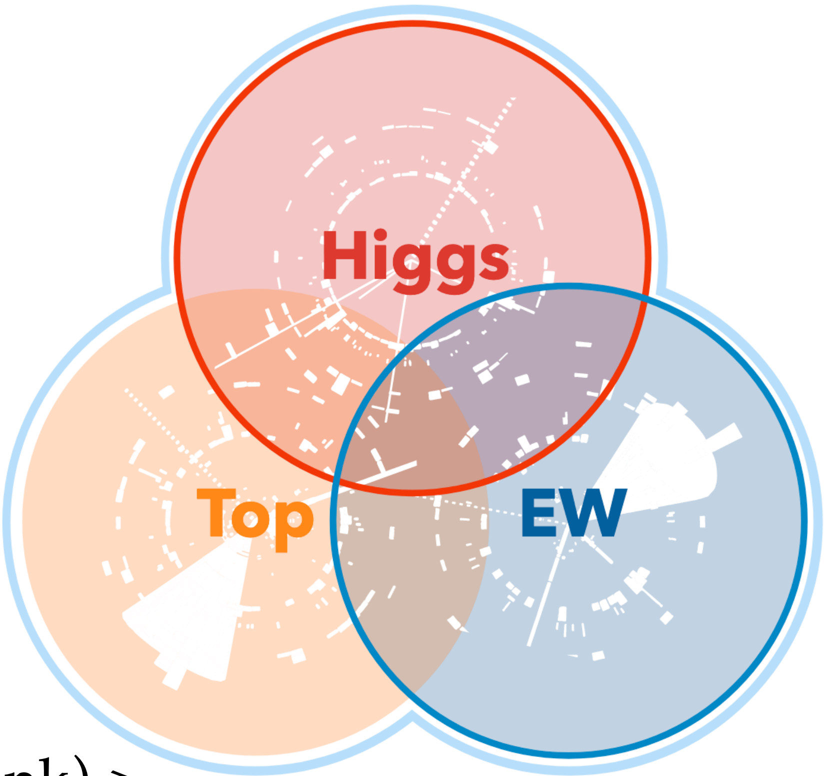

- Ongoing Higgs interpretation of STXS results from Nature Paper (Link)-> improvement expected coming from the inclusion of new inputs such as:
    - boosted-Hbb, $H \to Z\gamma$, $H \to c\bar{c}$, $H \to \mu\mu$.
    - "Top" flavour scheme to fully exploit all the channels included in the combination.
- Ongoing studies on the inclusion of dimension 8 terms and mapping EFT and UV theories.

- ATLAS + CMS: ongoing exercise to include few channels and test the combination using consistent parameterisations and assumptions-> developing tools for EFT parameterisation (further details in Fabian's talk)

Stay tuned for many interesting results to come!!

Thanks for your attention!

Evidence for the charge asymmetry in $pp \rightarrow t\bar{t}$

arXiv:2208.12095

- Inclusive and differential full Run2 measurements of the top–antitop ($t\bar{t}$) charge asymmetry $A_c^{t\bar{t}}$ and the leptonic asymmetry $A_c^{\ell\bar{\ell}}$
- Differential measurements are performed as a function of the invariant mass, transverse momentum and longitudinal boost of the $t\bar{t}$ system.
- Combined results are interpreted in the SMEFT framework.
- **14 four-fermion operators** + 1 operator for top–gluon interaction.

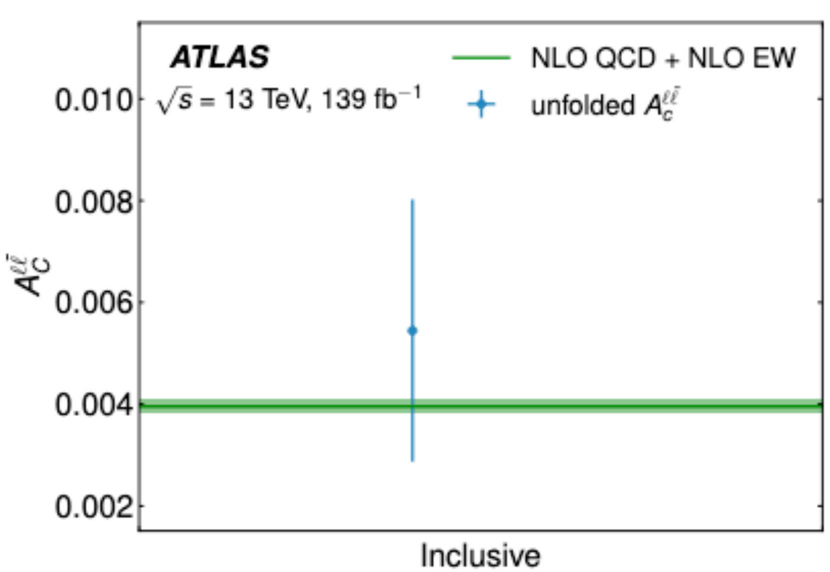

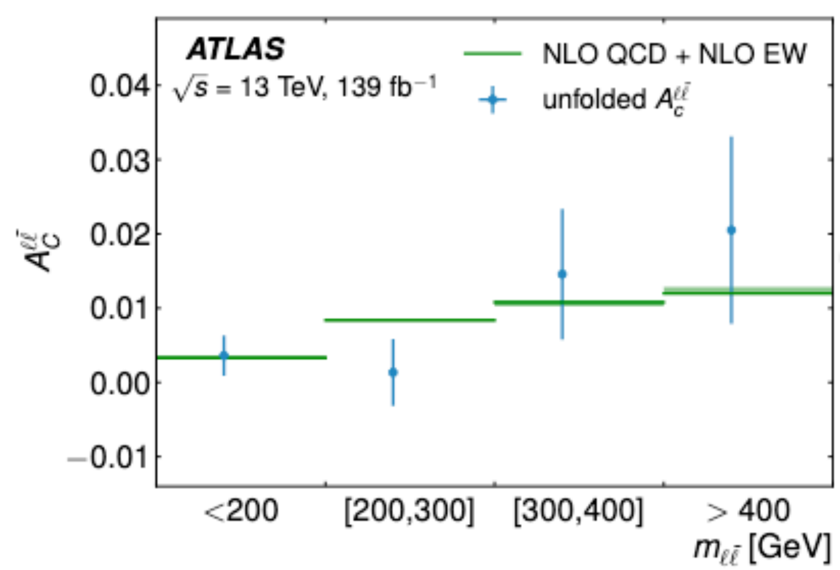

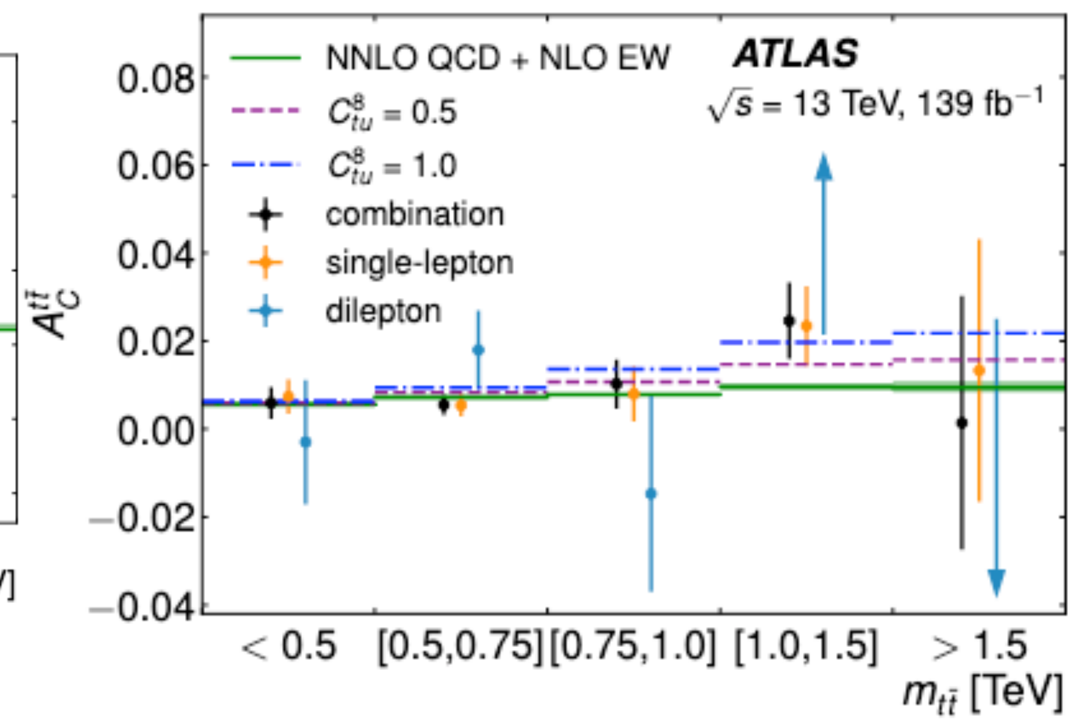

The combined inclusive charge asymmetry is measured to be $A_c^{t\bar{t}}$= 00068 ± 00015, which differs from zero by **4.7 standard deviations.**

Evidence for the charge asymmetry in $pp \to t\bar{t}$

arXiv:2208.12095

- Inclusive and differential full Run2 measurements of the top–antitop ($t\bar{t}$) charge asymmetry $A_c^{t\bar{t}}$ and the leptonic asymmetry $A_c^{\ell\bar{\ell}}$
- Differential measurements are performed as a function of the invariant mass, transverse momentum and longitudinal boost of the $t\bar{t}$ system.
- Combined results are interpreted in the SMEFT framework.
- **14 four-fermion operators** + 1 operator for top–gluon interaction.

- Large improvement comparing with LHC 8TeV / Tevatron results.
- Interplay between sensitivity, which increases rapidly at higher $m_{t\bar{t}}$, and uncertainty, which grows from 0.2%–0.3% in the lowest mass bin to 2.9% in the highest bin.
- For the linear fit, the tightest limit is obtained in the mass bin from 1 to 1.5 TeV.
- Constraint from the differential $m_{t\bar{t}}$ measurement more than a factor 2 stronger than the one from inclusive measurement (increase in sensitivity with higher $m_{t\bar{t}}$).

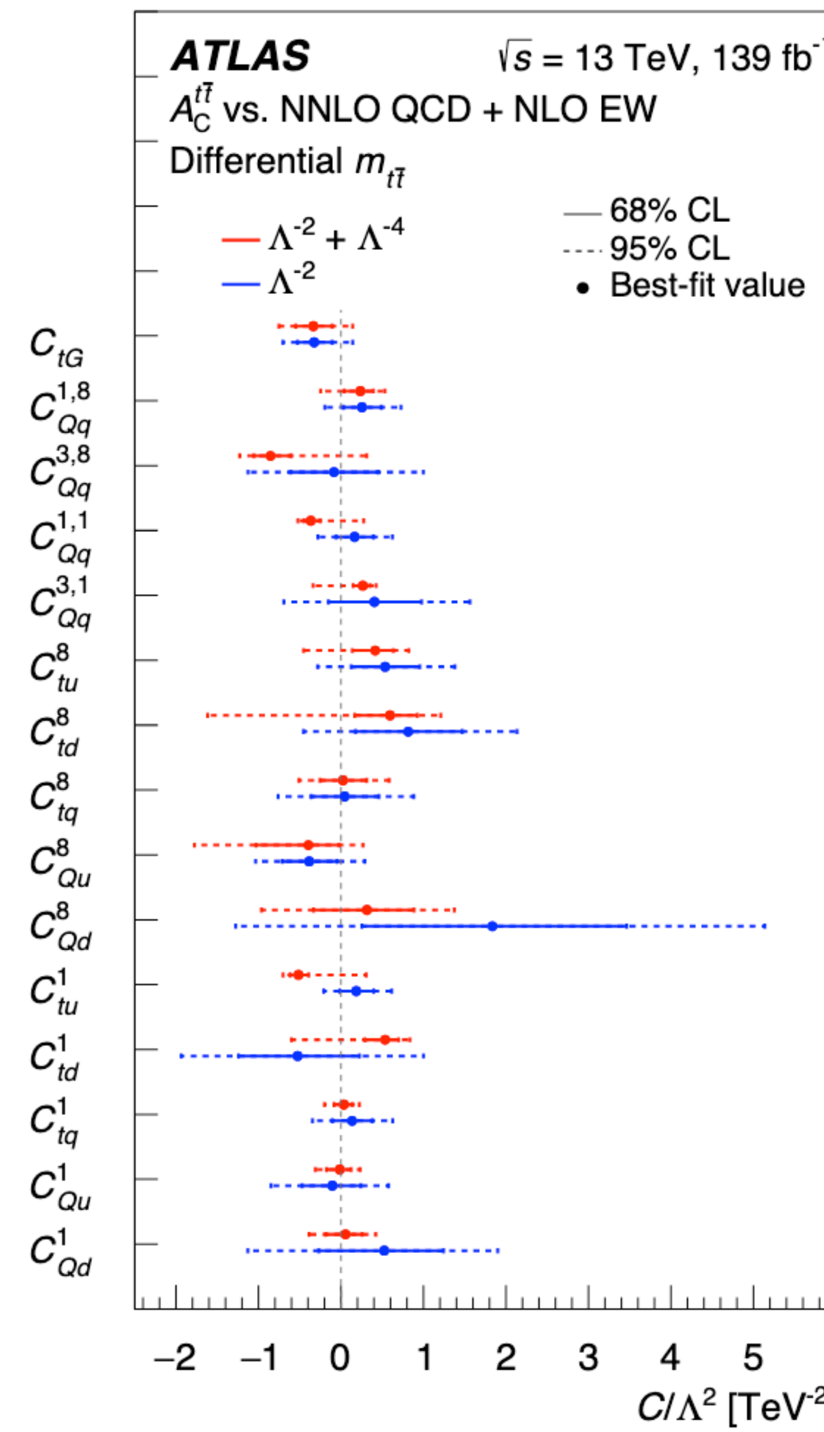

Individual 68% (solid line) and 95% (dashed line) CL limits on the Wilson coefficient

The combined inclusive charge asymmetry is measured to be $A_c^{t\bar{t}}$= 00068 ± 00015, which differs from zero by **4.7 standard deviations.**

Evidence for the charge asymmetry in $pp \rightarrow t\bar{t}$

arXiv:2208.12095

- Due to the extra jet in $t\bar{t}j$ production, the QCD structure of the energy asymmetry is not the same as for the charge asymmetry in $t\bar{t}$ production, so the two asymmetries probe different directions in chiral and colour space.
- For colour-singlet operators with different quark chiralities (top row), the two asymmetries probe similar areas in the parameter space.

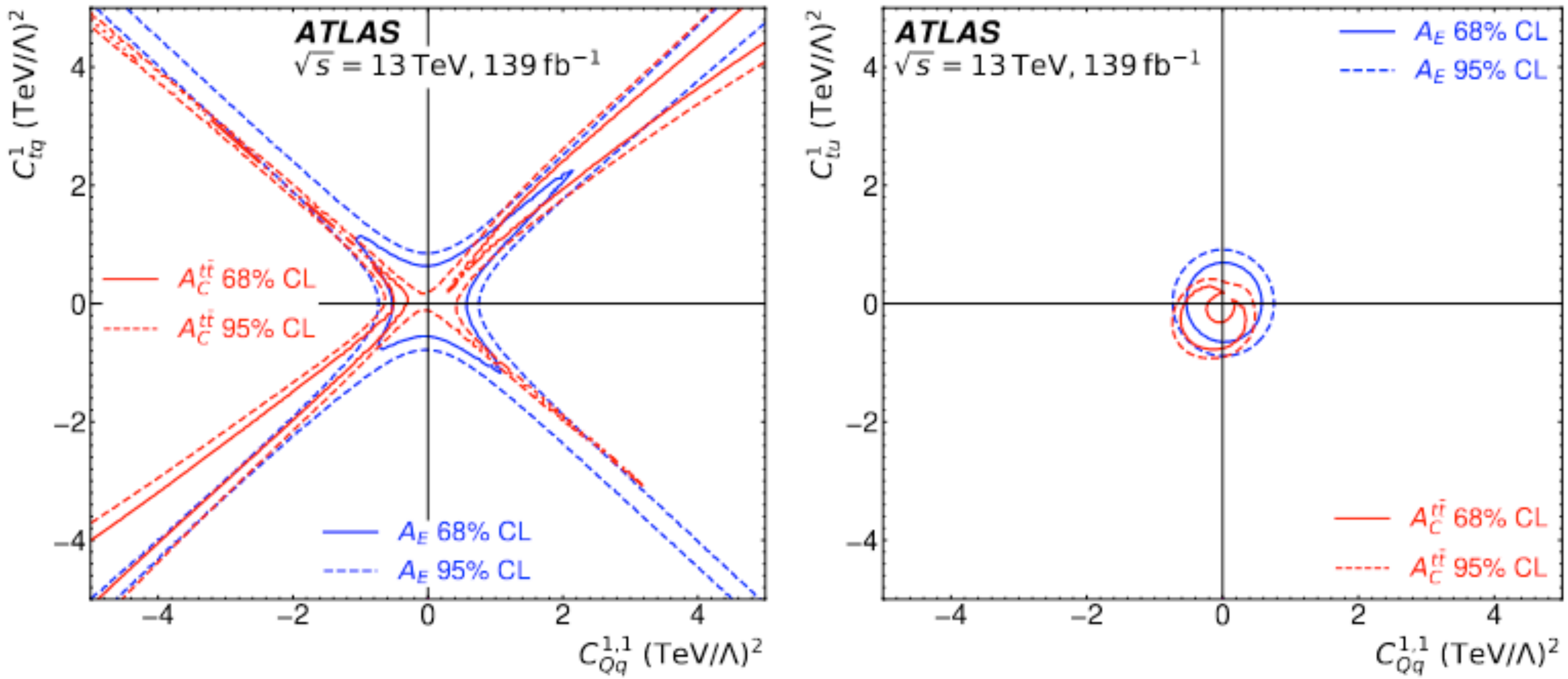

Evidence for the charge asymmetry in $pp \to t\bar{t}$

arXiv:2208.12095

- Due to the extra jet in $t\bar{t}j$ production, the QCD structure of the energy asymmetry is not the same as for the charge asymmetry in $t\bar{t}$ production, so the two asymmetries probe different directions in chiral and colour space.
- The bottom row shows. Here, the different shapes of the bounds are due to the different colour-singlet and colour-octet contributions to $t\bar{t}$ and $t\bar{t}j$ production, which is probed with high sensitivity by the asymmetries.

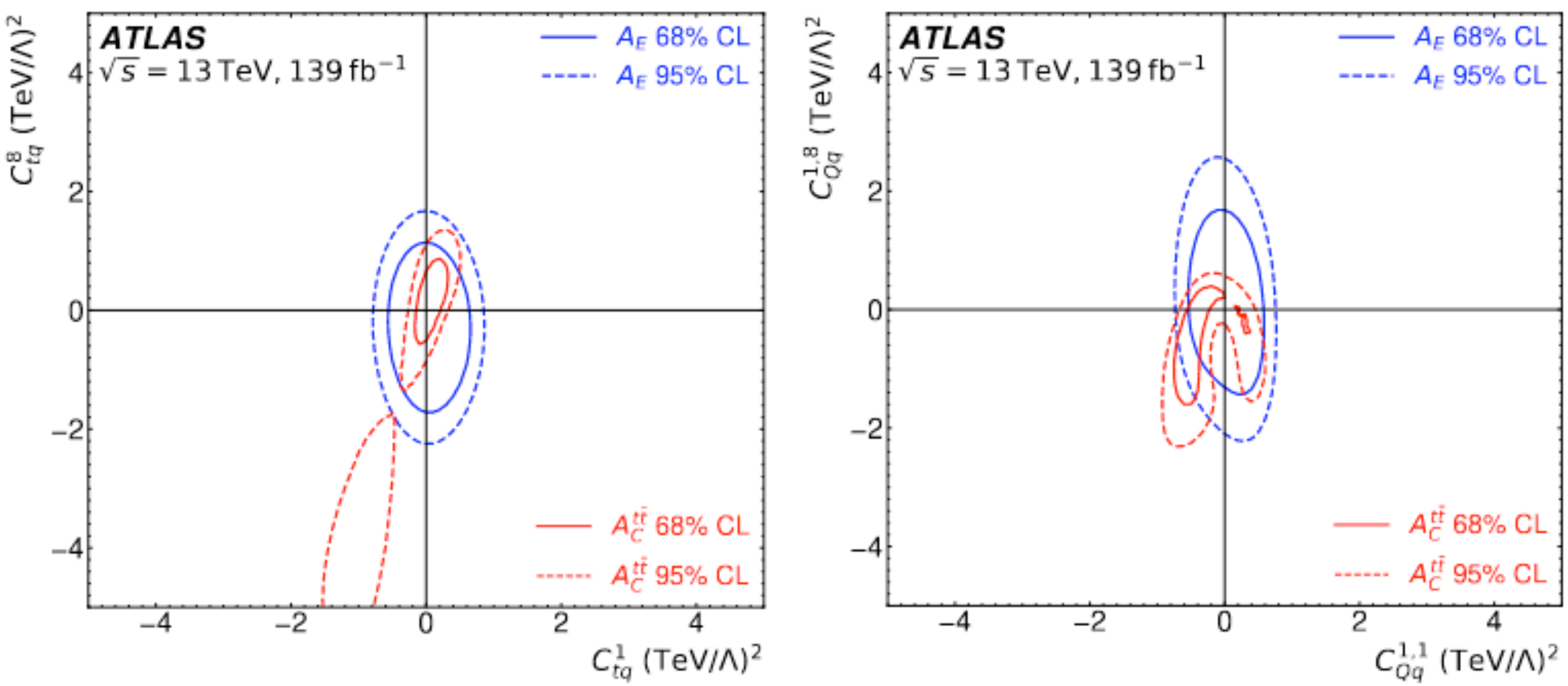

colour-singlet versus colour-octet operators with the same quark chiralities

New SMEFTsim v3.0

	general		U35		MFV		top		topU31	
	all	~~CP~~	all	~~CP~~	all	~~CP~~	all	~~CP~~	all	~~CP~~
$\mathcal{L}_6^{(1)}$	4	2	4	2	2	-	4	2	4	2
$\mathcal{L}_6^{(2,3)}$	3	-	3	-	3	-	3	-	3	-
$\mathcal{L}_6^{(4)}$	8	4	8	4	4	-	8	4	8	4
$\mathcal{L}_6^{(5)}$	54	27	6	3	7	-	14	7	10	5
$\mathcal{L}_6^{(6)}$	144	72	16	8	20	-	36	18	28	14
$\mathcal{L}_6^{(7)}$	81	30	9	1	14	-	21	2	15	2
$\mathcal{L}_6^{(8a)}$	297	126	8	-	10	-	31	-	16	-
$\mathcal{L}_6^{(8b)}$	450	195	9	-	19	-	40	2	27	2
$\mathcal{L}_6^{(8c)}$	648	288	8	-	28	-	54	4	31	4
$\mathcal{L}_6^{(8d)}$	810	405	14	7	13	-	64	32	40	20
tot	2499	1149	85	25	120	-	275	71	182	53

From Ilaria's talk

SMEFT parameterisation

The impact of dim-6 CP-even operators is estimated using both MC truth and analytical predictions for all the Wilson coefficients that have numerically relevant contributions (62).

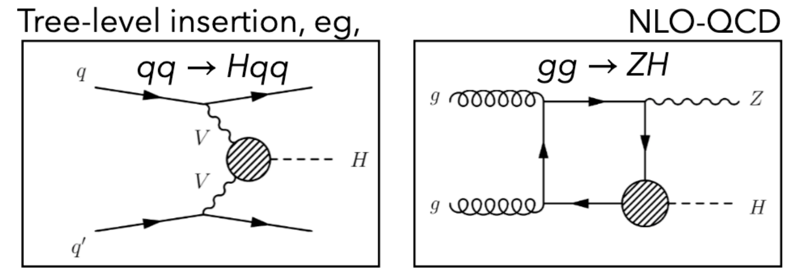

- Dimension-six operator effects are calculated:
  - at tree level using SMEFTsim 3.0.
  - for processes that are loop-induced in the SM, thus ggH and ggZH production, Higgs boson decays into gluons -> SMEFTatNLO.
  - Analytic formulas for $H \to \gamma\gamma$ including NLO EW corrections and LEP observables.
- Theory uncertainties on SM predictions, no additional uncertainties on SMEFT.
- Acceptance corrections to account for kinematic differences between SM and SMEFT in Higgs boson decays on both **linear** and **linear+quadratic** terms.
- Effects of width changes of intermediate particles ("propagator corrections") included.

SMEFT interpretation workflow

Parameterisation

CERN-EP-2022-094

Relative Impact w.r.t SM

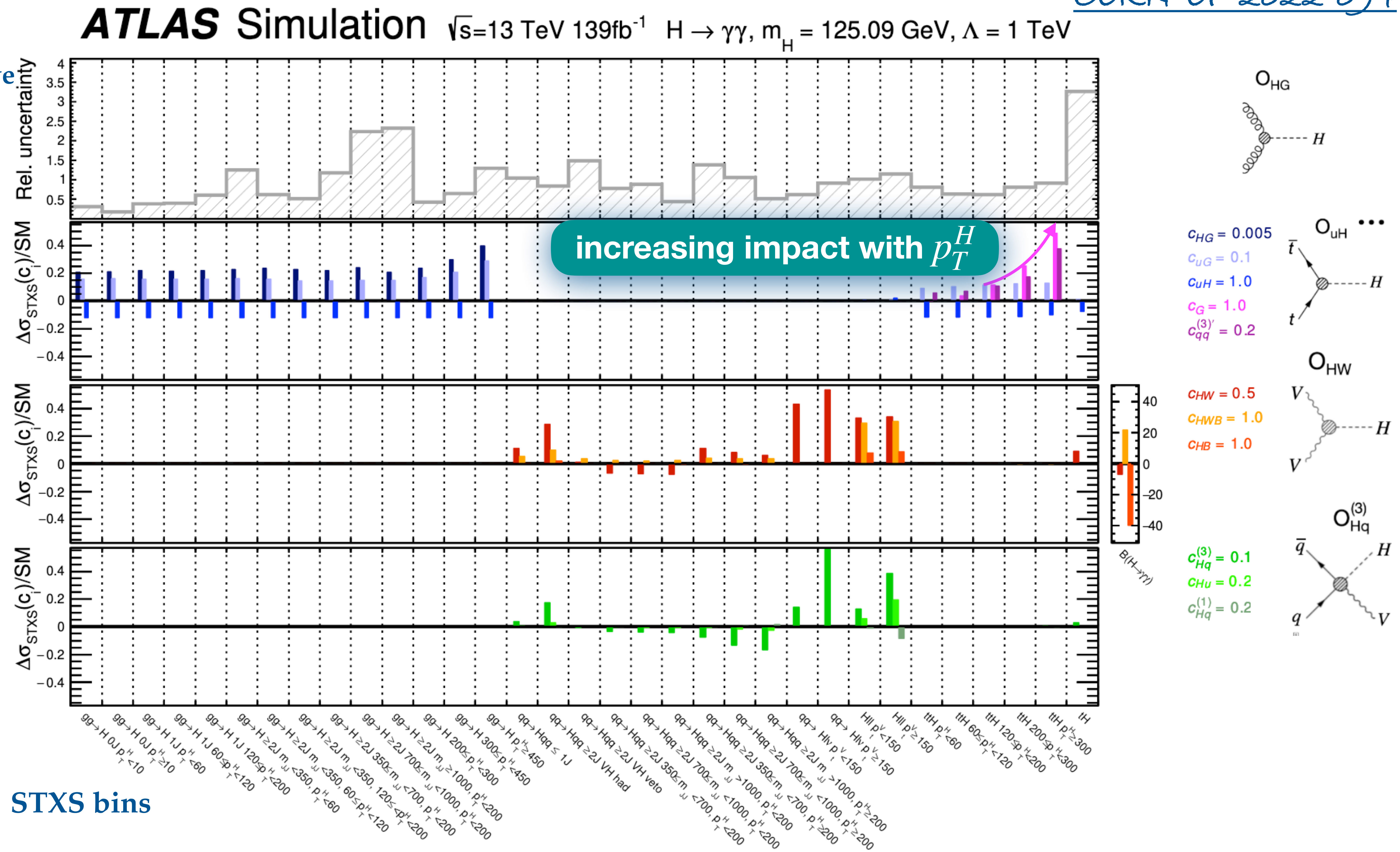

STXS bins

$H \rightarrow \gamma\gamma$: constraints on sensitive directions

CERN-EP-2022-094

- Operators grouped according to the eigenvectors of the information matrix of the measurement.
- All results are in agreement with SM expectations.

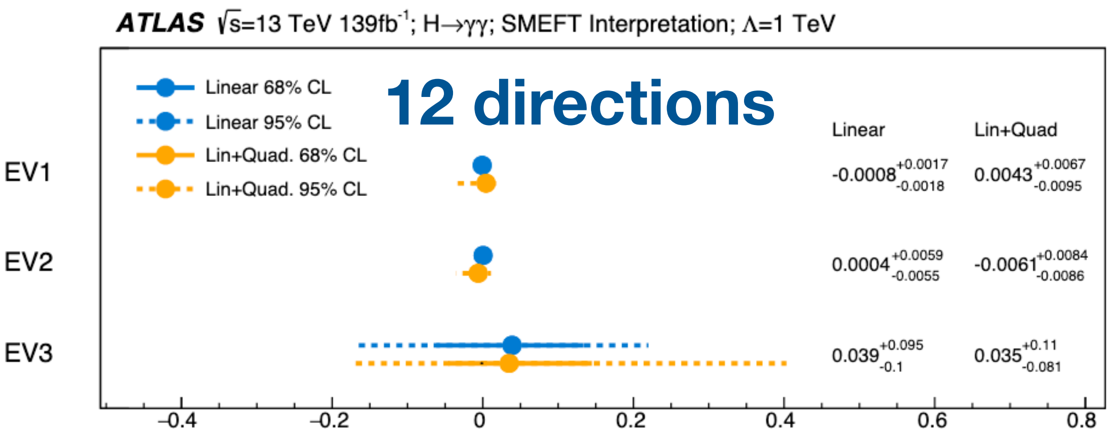

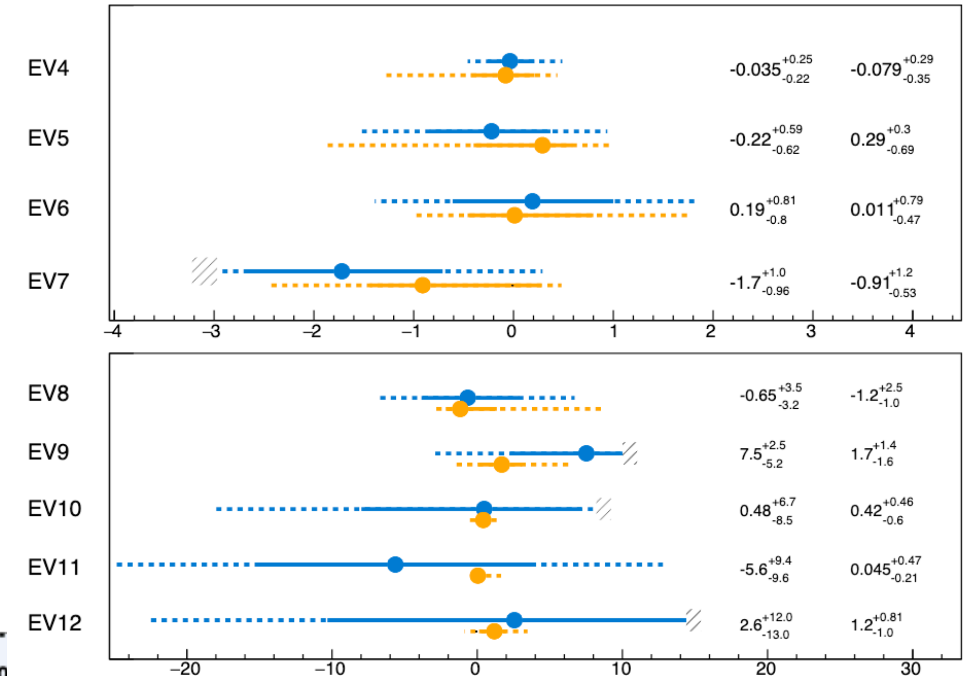

ATLAS √s=13 TeV 139fb⁻¹; H→γγ

	c_{HG}	c_{uG}	c_{uH}	c_{HW}	c_{HB}	c_{HWB}	c_{W}	c_{uW}	c_{uB}	$c^{(3)}_{Hl}$	c'_{ll}	c_{HDD}	c_{Hbox}	$c^{(3)}_{Hq}$	c_{Hu}	c_{Hd}	$c^{(1)}_{Hq}$
EV12	-0.00	-0.01	-0.15	0.01	-0.20	-0.36	-0.00	0.02	-0.01	-0.13	-0.16	-0.06	0.00	-0.00	0.37	-0.30	0.69
EV11	0.00	-0.01	0.04	0.01	-0.03	-0.05	-0.00	-0.02	0.00	-0.10	0.03	-0.00	0.00	0.00	0.06	-0.05	0.11
EV10	-0.00	-0.00	0.06	0.02	-0.09	-0.13	-0.00	0.37	-0.00	0.05	-0.02	-0.00	0.00	-0.00	0.01	0.02	-0.14
EV9	-0.00	0.01	0.03	0.09	-0.38	-0.65	-0.00	-0.08	-0.01	-0.17	0.03	-0.08	0.00	-0.02	0.13	0.04	-0.56
EV8	-0.00	0.27	0.38	0.02	0.06	0.10	0.00	0.02	0.00	-0.78	0.37	0.07	-0.00	0.01	-0.04	0.00	0.09
EV7	-0.00	0.03	0.03	0.09	0.15	0.32	0.00	0.00	0.00	0.02	0.01	0.05	0.00	-0.10	0.83	-0.25	-0.31
EV6	0.01	-0.24	0.01	-0.90	0.21	-0.14	0.01	0.01	0.01	-0.11	0.01	0.01	-0.00	0.15	0.10	-0.03	-0.08
EV5	-0.02	0.64	-0.09	-0.24	0.04	-0.06	0.00	0.00	0.00	0.15	-0.09	-0.01	-0.00	0.05	0.02	-0.01	-0.02
EV4	-0.01	0.68	-0.06	-0.08	0.01	-0.04	0.00	-0.01	-0.00	0.13	-0.07	-0.01	0.00	0.08	0.00	-0.00	-0.01
EV3	-0.01	0.05	-0.01	-0.17	0.03	-0.04	0.00	0.00	0.00	-0.01	-0.01	0.00	-0.00	-0.98	-0.07	0.02	0.03
EV2	-0.85	-0.02	0.00	-0.14	-0.44	0.25	-0.01	-0.01	-0.02	-0.01	0.00	-0.00	0.00	0.01	0.00	-0.00	-0.00
EV1	-0.53	-0.02	0.00	0.23	0.71	-0.40	0.02	0.02	0.04	0.01	-0.00	0.00	-0.00	-0.00	-0.00	0.00	0.00

	c_{He}	$c^{(1)}_{Hl}$	c_{G}	$c^{(1)}_{qq}$	$c^{(1)'}_{qq}$	$c^{(3)}_{qq}$	$c^{(3)'}_{qq}$	c_{uu}	c'_{uu}	$c^{(8)}_{ud}$	$c^{(1)}_{qu}$	$c^{(8)}_{qu}$	$c^{(8)}_{qd}$	$c^{(1)}_{ud}$	c_{eH}	c_{dH}	
EV12	0.10	0.14	0.14	[illegible]	[illegible]	[illegible]	[illegible]	[illegible]	[illegible]	[illegible]	[illegible]	[illegible]	[illegible]	[illegible]	[illegible]	[illegible]	0.0067
EV11	0.01	0.02	-0.95	-0.00	0.15	0.05	0.11	-0.01	0.13	-0.01	-0.01	0.09	-0.00	0.00	-0.00	0.00	λ =0.0108
EV10	0.02	0.03	-0.05	0.00	0.04	-0.89	0.06	0.00	0.03	0.00	-0.00	0.02	0.00	0.00	0.00	0.00	λ =0.027
EV9	0.09	0.12	0.02	-0.00	-0.01	0.18	-0.02	-0.00	-0.01	-0.00	-0.00	-0.01	-0.00	-0.00	-0.00	0.00	λ =0.038
EV8	0.00	0.00	0.09	-0.00	-0.03	-0.06	-0.04	0.00	-0.03	0.00	0.00	-0.02	-0.00	-0.00	-0.00	-0.00	λ =0.075
EV7	-0.04	-0.05	0.00	0.00	0.00	-0.01	0.00	0.00	0.00	-0.00	0.00	0.00	-0.00	-0.00	-0.00	0.00	λ =0.89
EV6	0.00	0.01	0.03	0.00	0.05	0.00	0.08	0.00	0.05	0.00	0.00	0.03	0.00	-0.00	-0.00	-0.00	λ =1.78
EV5	0.00	0.00	-0.19	-0.02	-0.28	-0.04	-0.52	-0.01	-0.27	-0.03	-0.01	-0.16	-0.03	0.00	-0.00	-0.00	λ =2.87
EV4	0.00	0.00	0.14	0.01	0.27	0.06	0.56	0.02	0.26	0.04	0.01	0.17	0.04	-0.00	-0.00	0.00	λ =20.2
EV3	0.00	0.00	0.01	0.00	0.01	0.00	0.03	0.00	0.01	0.00	0.00	0.01	0.00	-0.00	0.00	-0.00	λ =106
EV2	-0.00	-0.00	0.00	0.00	0.00	0.00	0.01	0.00	0.00	0.00	0.00	0.00	0.00	-0.00	0.00	0.00	λ =34473
EV1	-0.00	-0.00	-0.00	0.00	-0.00	-0.00	-0.00	0.00	-0.00	-0.00	0.00	-0.00	-0.00	-0.00	-0.00	-0.00	λ =346827

Electroweak precision observables

- Electroweak precision observables (EWPO) measured e.g. at LEP and SLC, including 8 observables in our fit.
- Constraints obtained from the interpretation of these observables are typically more precise than LHC constraints but only a limited number of directions in parameter space can be constrained.
- The tight EWPO constraints provided on operators affecting weak-boson–fermion couplings allow to **disentangle** their effect from those affecting only Higgs or weak-boson self couplings, which cannot be constrained with Z-pole data.
- The precision observables agree very well with the SM expectation, with the exception of $A_{FB}^{0,b}$ and $A_{FB}^{0,c}$ for which deviations of more than three and more than one standard deviations, respectively, are found.
- Linear only parameterisation.

Example of linear parameterisation for EWPO observables

$$\frac{\Gamma_Z}{\Gamma_{Z,\mathrm{SM}}} = 1 + 0.059c_{ll}^{(1)} - 0.004c_{Hb} - 0.004c_{HD} - 0.007c_{Hd} - 0.011c_{Hl}^{(1)} - 0.081c_{Hl}^{(3)} - 0.011c_{He} + 0.007c_{Hq}^{(1)} + 0.021c_{HQ}^{(1)} + 0.075c_{Hq}^{(3)} + 0.021c_{HQ}^{(3)} + 0.014c_{Hu} + 0.027c_{HWB}$$

Observable	Measurement	Prediction	Ratio
Γ_Z [MeV]	2495.2 ± 2.3	2495.7 ± 1	0.9998 ± 0.0010
R_ℓ^0	20.767 ± 0.025	20.758 ± 0.008	1.0004 ± 0.0013
R_c^0	0.1721 ± 0.003	0.17223 ± 0.00003	0.999 ± 0.017
R_b^0	0.21629 ± 0.00066	0.21586 ± 0.00003	1.0020 ± 0.0031
$A_{\mathrm{FB}}^{0,\ell}$	0.0171 ± 0.0010	0.01718 ± 0.00037	0.995 ± 0.062
$A_{\mathrm{FB}}^{0,c}$	0.0707 ± 0.0035	0.07583 ± 0.00117	0.932 ± 0.048
$A_{\mathrm{FB}}^{0,b}$	0.0992 ± 0.0016	0.10615 ± 0.00162	0.935 ± 0.021
σ_{had}^0 [pb]	41488 ± 6	41489 ± 5	0.99998 ± 0.00019

ATLAS Global combination: acceptance

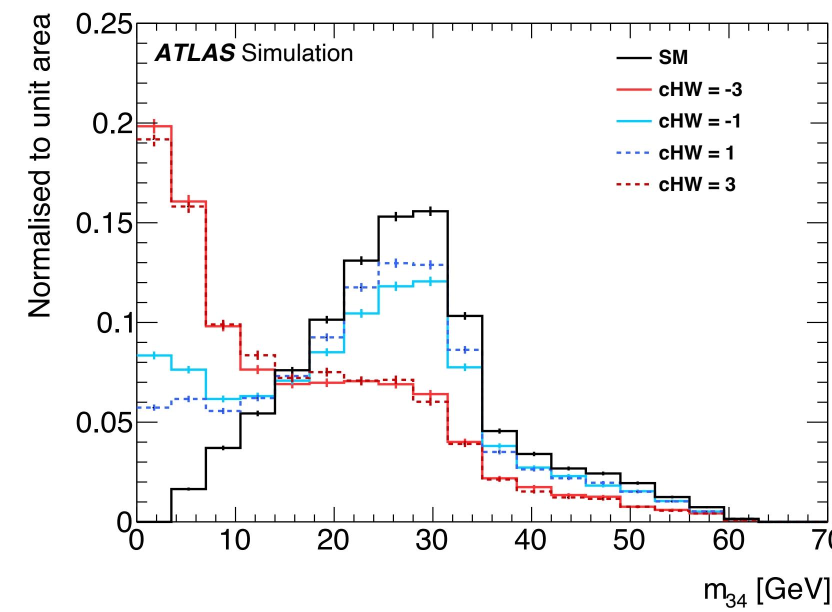

- EFT parameterisation is affected by analysis level selections used to reconstruct SM Higgs.
- Acceptance effect can be considerable when the shape of EFT distribution is different from the SM distribution.
- Assuming SM-like acceptance not always possible-> modifications for $H \to ZZ$ (ggH production - valid for all) and $H \to WW$ are considered.
- Example: shape of the invariant mass distribution of the secondary lepton pair in $H \to 4l$ decays for various values of the Wilson coefficients c_{HW} and c_{HB}.
- Acceptance parameterisation is a ratio of polynomials, linearised using Taylor expansion.

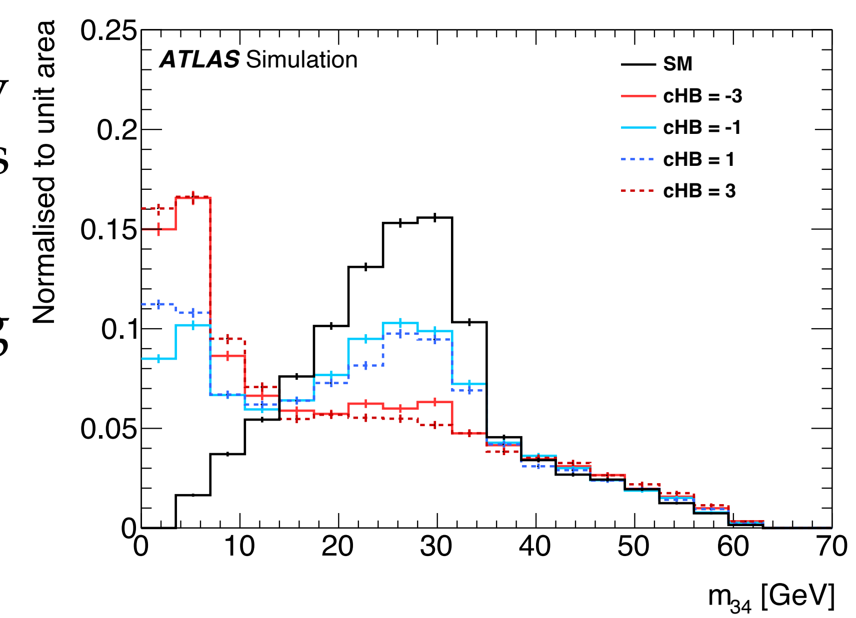

For one coupling, the acceptance can be approximated using a Taylor expansion:

$$\frac{A^{BSM}}{A^{SM}} = \frac{1 + a_{fid} c_i + b_{fid} c_i^2}{1 + a_{tot} c_i + b_{tot} c_i^2}$$

$$\approx 1 + (a_{fid} - a_{tot}) c_i + (b_{fid} - b_{tot} - a_{fid} a_{tot} + a_{tot}^2) c_i^2 + \ldots$$

ATLAS Global combination: statistical combination

- Overlapping categories:
  - regions of the inclusive 4ℓ analysis that target **$m_{4\ell}$ < 180 GeV are excluded** (small impact on SMEFT).
  - **the 0-jet WW control region from HWW is excluded**; WW normalisation is correlated with WW signal normalisation.
- A multivariate Gaussian model is used for the interpretation of both LHC EW measurements and EWPO.
- Systematic uncertainties modelled with common nuisance parameter:
  - for unfolded SM measurements: experimental nuisance parameter shift unfolded results;
  - same nuisance parameter shift reco-level prediction for Higgs measurements.
- For EWPO the model contains no nuisance parameters and both theoretical and experimental uncertainties are included in the covariance matrix.
- Limits on WCs extracted using combined likelihood (product of individual likelihood) .

Correlated Uncertainty Source	Parameters
Luminosity (correlated part)	1
Luminosity 2015/16	1
Luminosity 2017/18	1
Pile-up modelling	1
Pile-up jet suppression	1
Jet energy scale (pile-up modelling)	3
Jet energy scale η-inter-calibration	1
Jet energy resolution	12
B-tagging efficiency (WW and $H \to WW^*$)	1
WW modelling (WW and $H \to WW^*$)	2

ATLAS Global combination

Impact of linear SMEFT parameterisation shown for bins along with corresponding measurement uncertainty

- Relative impact of linear SMEFT terms with Wilson coefficients c_{HG}, c_W, c_{tG}, c_{bH}, c_{tH}, and c_{eH} on the Higgs STXS cross sections and branching ratios.

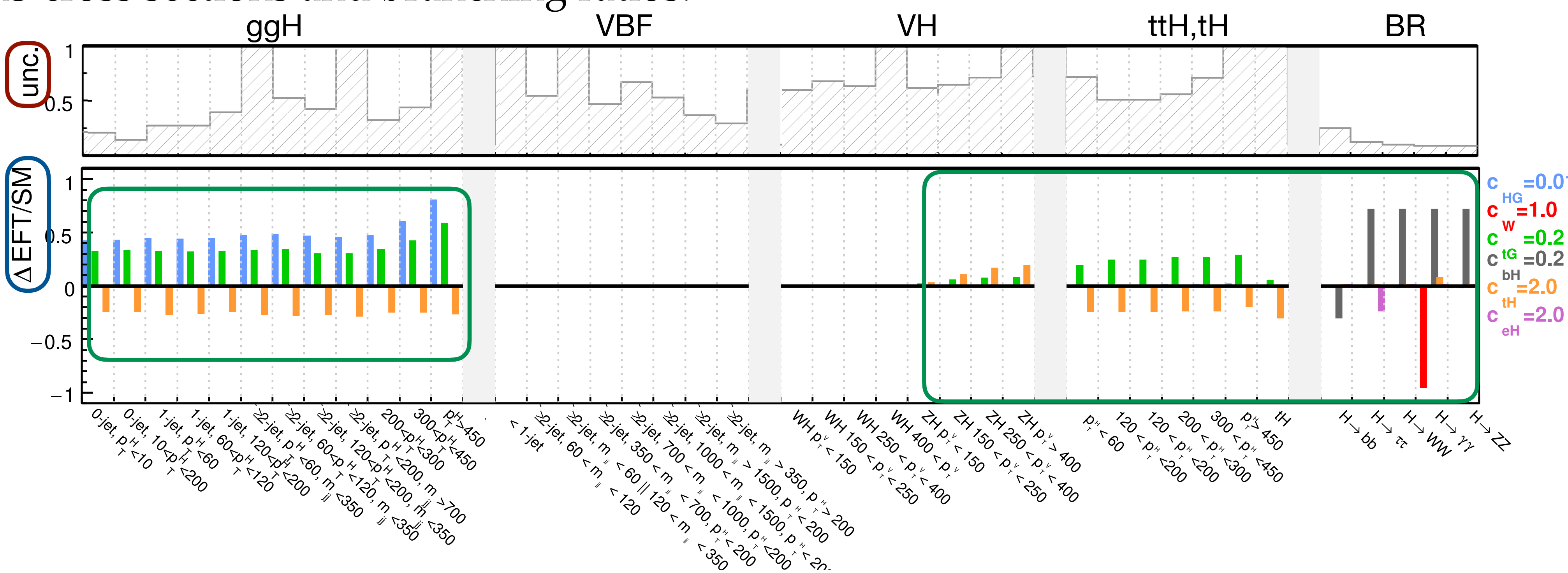

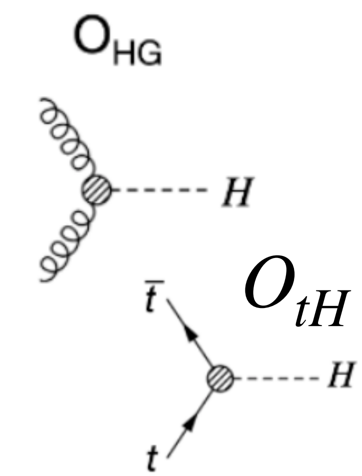

The corresponding selected values of Wilson coefficients are shown

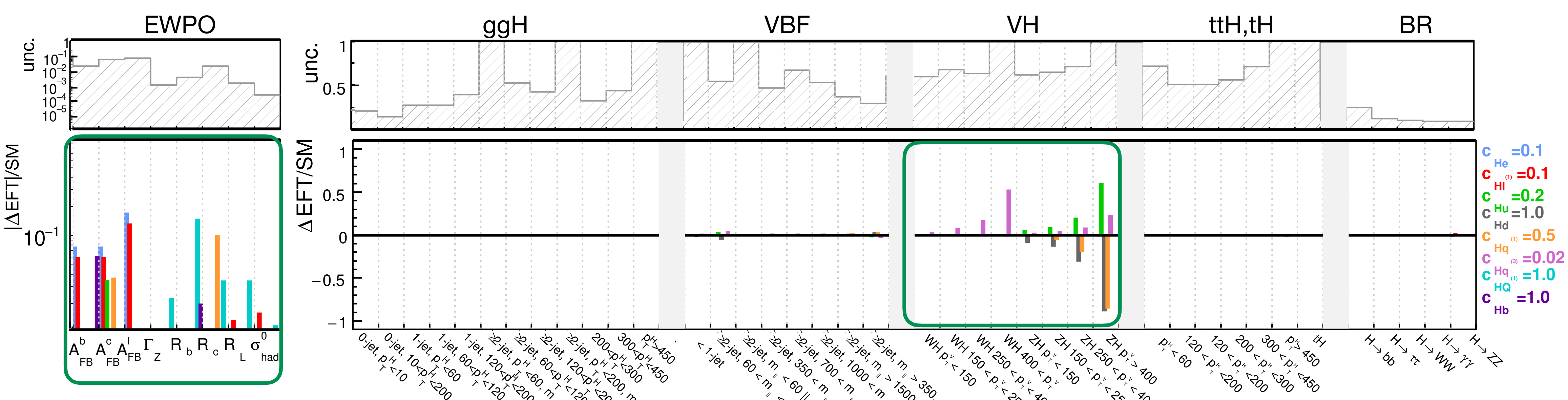

operators affecting HVV,Vff

ATL-PHYS-PUB-2022-037

ATLAS Global combination

- Additional sensitivity coming from EW measurements and EWPO, e.g. cW that cannot be disentangled using just $H \rightarrow \gamma\gamma$ decay.

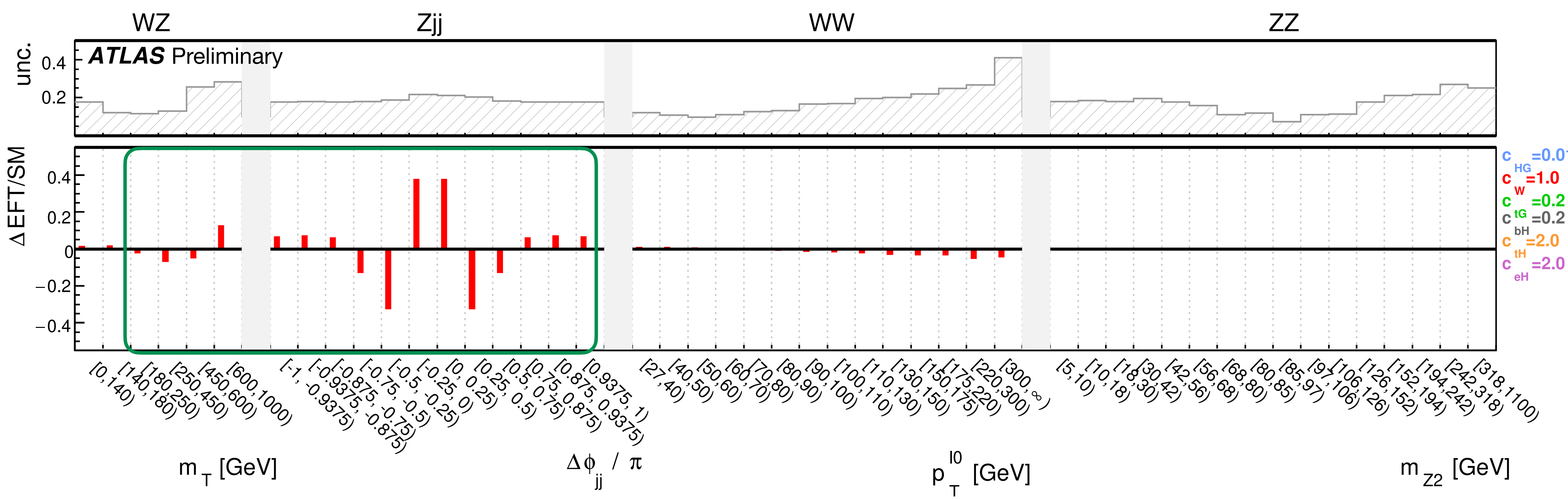

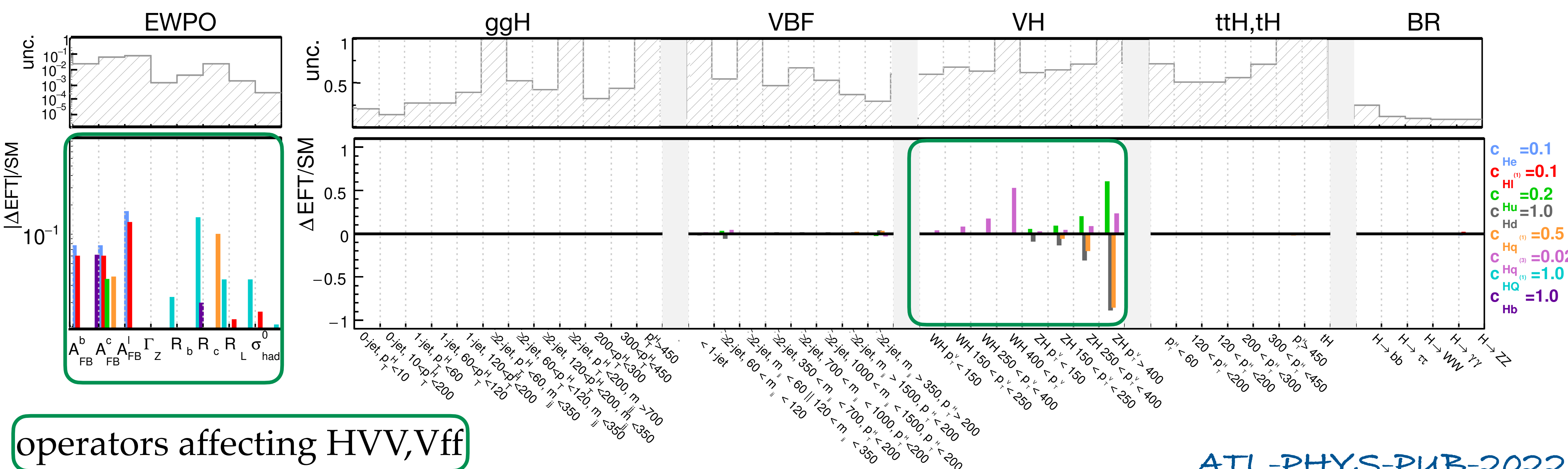

ATL-PHYS-PUB-2022-037

ATLAS Global combination

Impact of linear SMEFT parameterisation shown for bins along with corresponding measurement uncertainty

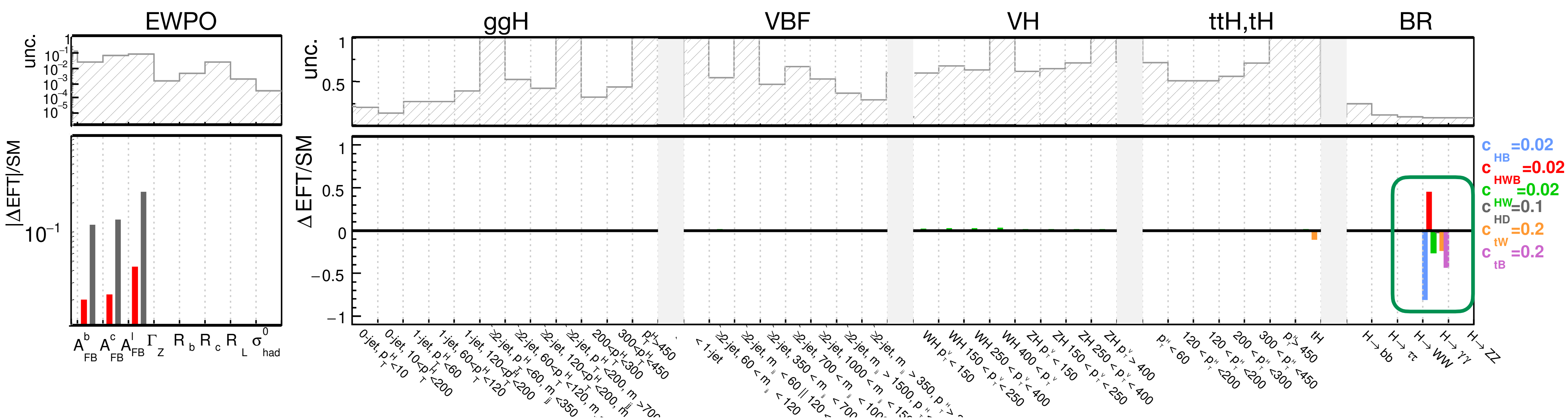

mostly affecting the $H \to \gamma\gamma$ branching ratio

O_{HW}

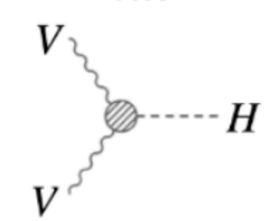

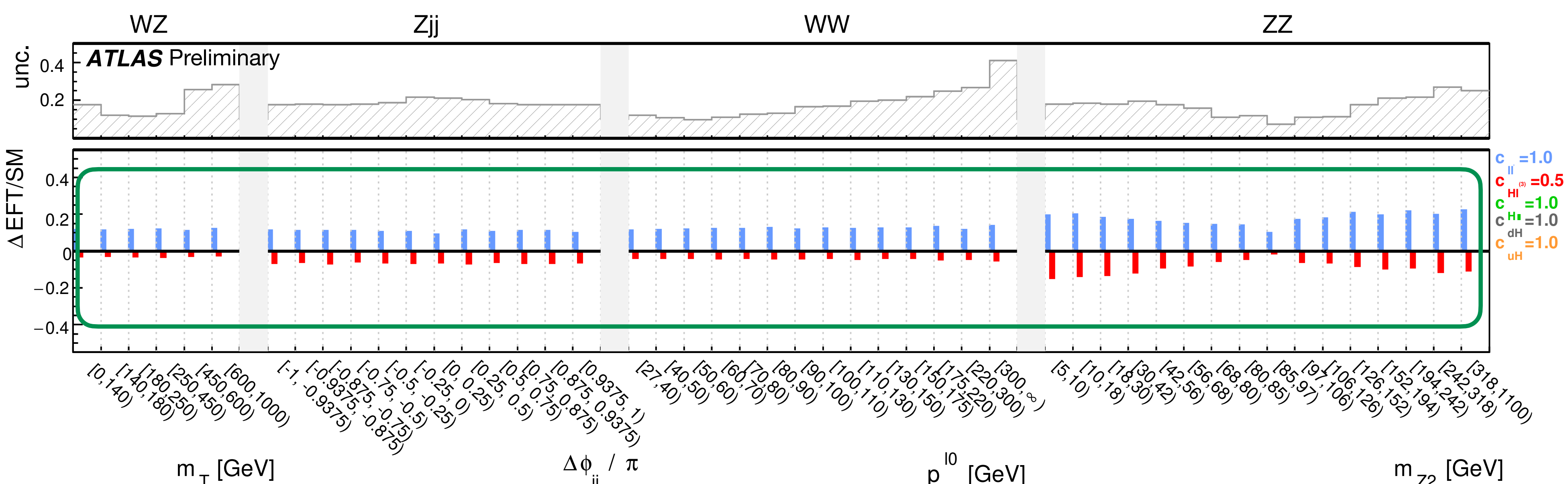

overall normalisation, modifications to Fermi constant (cHl3, cll1)

ATL-PHYS-PUB-2022-037

ATLAS Global combination

- SMEFT impact on measurements shown in Warsaw basis and fit basis-> allows to understand the impact of the different fit directions on measurements.

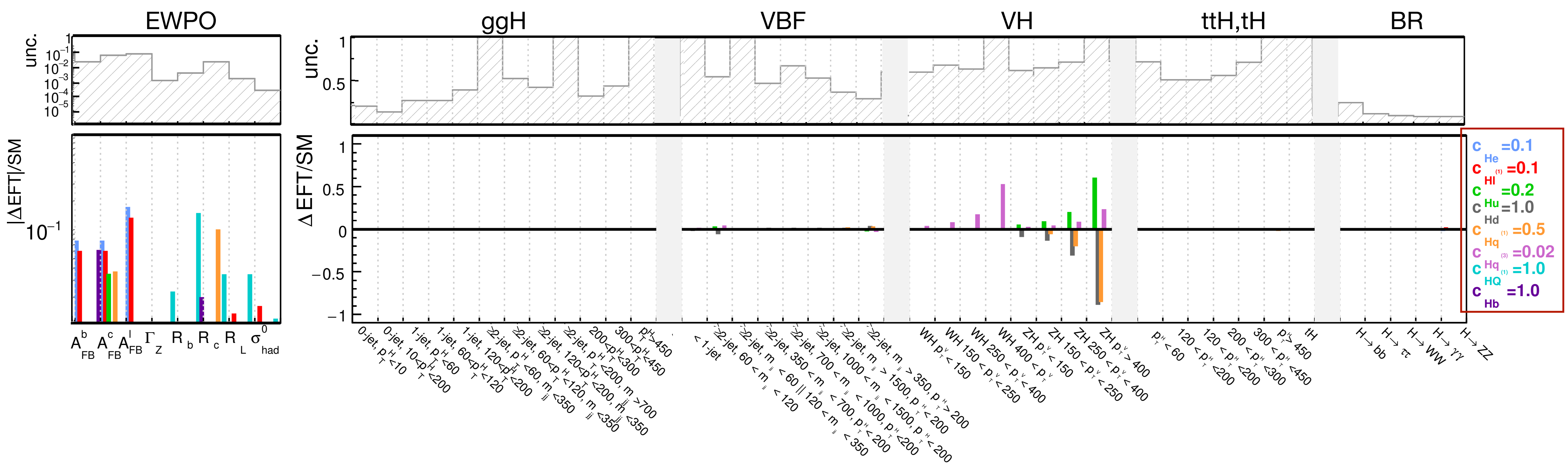

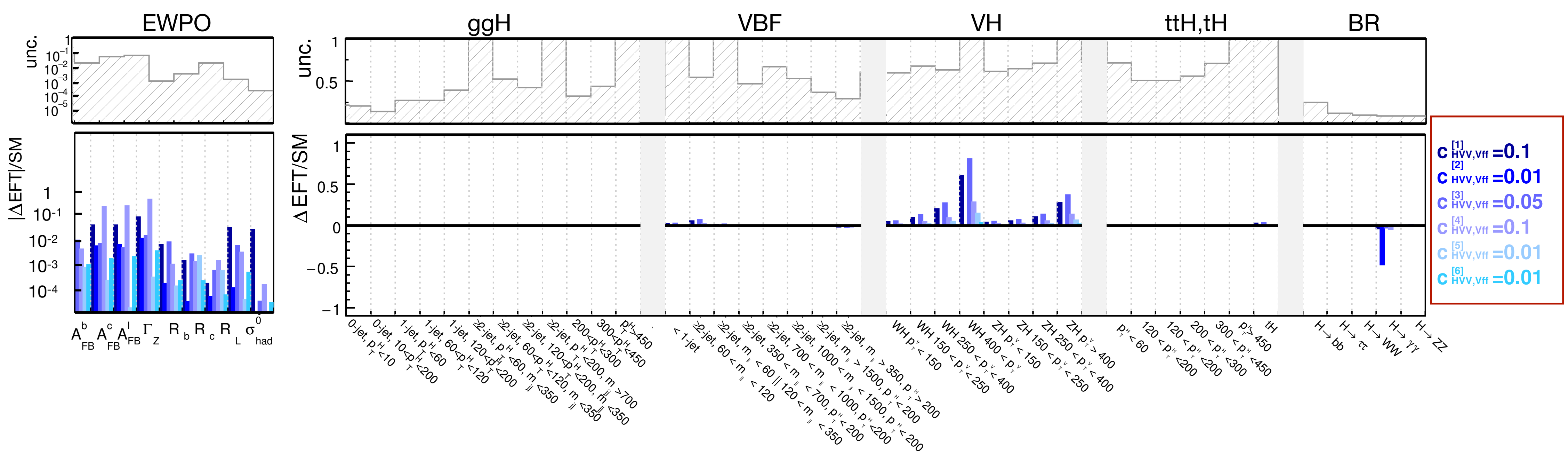

ATLAS Global combination: sensitivity studies

- Principal Component Analysis to reduce the dimensionality of the fit. ATL-PHYS-PUB-2022-037
- A simultaneous measurement of the signal strengths in each measurement bin is performed using a maximum likelihood fit exploiting a signal strength parameter μ_b:

$$1 + \sum_i A_{bi} c_i + \sum_i B_{bi} c_i^2 + \sum_{i<j} C_{bij} c_i c_j \rightarrow \mu_b$$

- The Hessian matrix H_μ at the minimum of the negative log likelihood of the μ_b measurement is reparameterised in terms of Wilson coefficients using the linear parameterisation matrix P.
- H_{SMEFT}, can be obtained from the Hessian matrix H_μ in μ_b space:

$$H_{SMEFT} = P^T H_\mu P$$

- P: matrix that gives the parametrisation of the observables as a function of the Wilson coefficients;
- $A_i^{b_j}$: factors obtained from the simulation.

$$P = \begin{pmatrix} A_0^{b_0} & A_1^{b_0} & A_2^{b_0} & \dots \\ A_0^{b_1} & A_1^{b_1} & A_2^{b_1} & \dots \\ A_0^{b_2} & A_1^{b_2} & A_2^{b_2} & \dots \\ \vdots & \vdots & \vdots & \end{pmatrix}$$

SMEFTsim

SMEFT@NLO

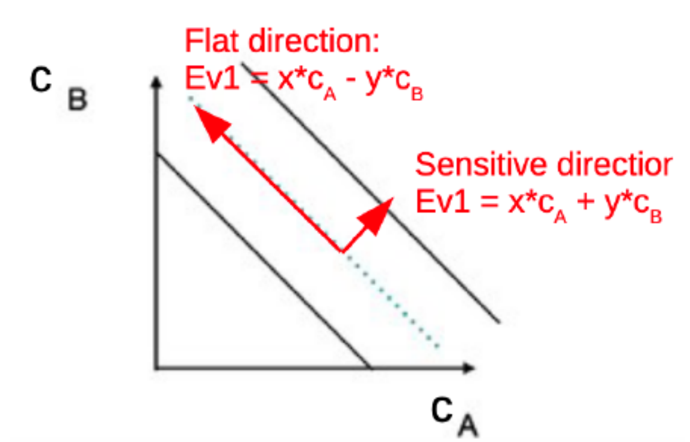

ATLAS Global combination: sensitivity studies

- PCA considering all operators: directions ordered by increasing uncertainties, keeping $\sigma < 5$;
- Wilson coefficients expected to be at most order 1, new physics scale Λ expected to be at least 1 TeV -> directions with $\sigma > 5$ have very little impact on the measurement.

Eigenvectors from PCA, corresponding eigenvalues

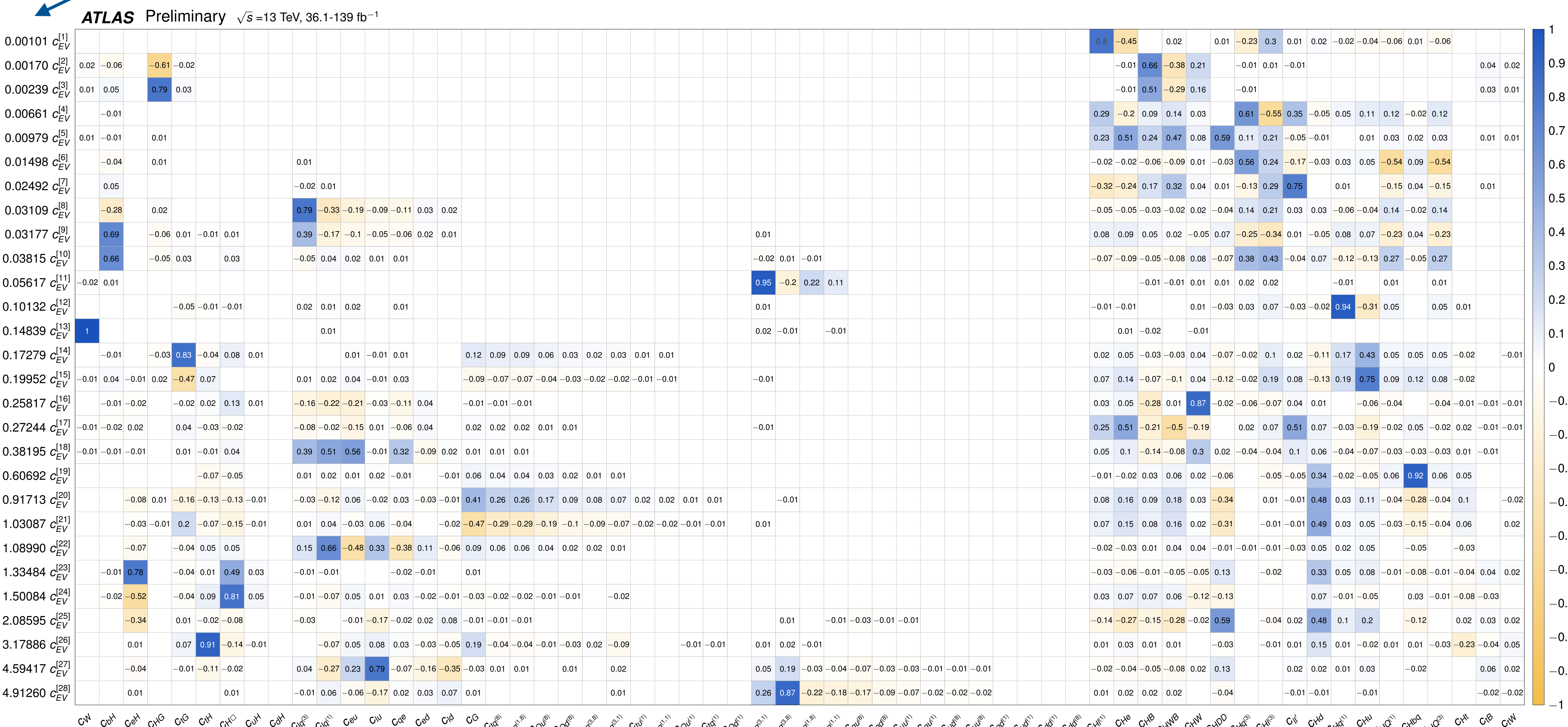

ATL-PHYS-PUB-2022-037 **Warsaw Basis, Wilson coefficients**

ATLAS Global combination: sensitivity studies

ATL-PHYS-PUB-2022-037

- PCA considering all operators: directions ordered by increasing uncertainties, keeping $\sigma < 5$;
- Fit basis defined by grouping operators of similar physics impact together.

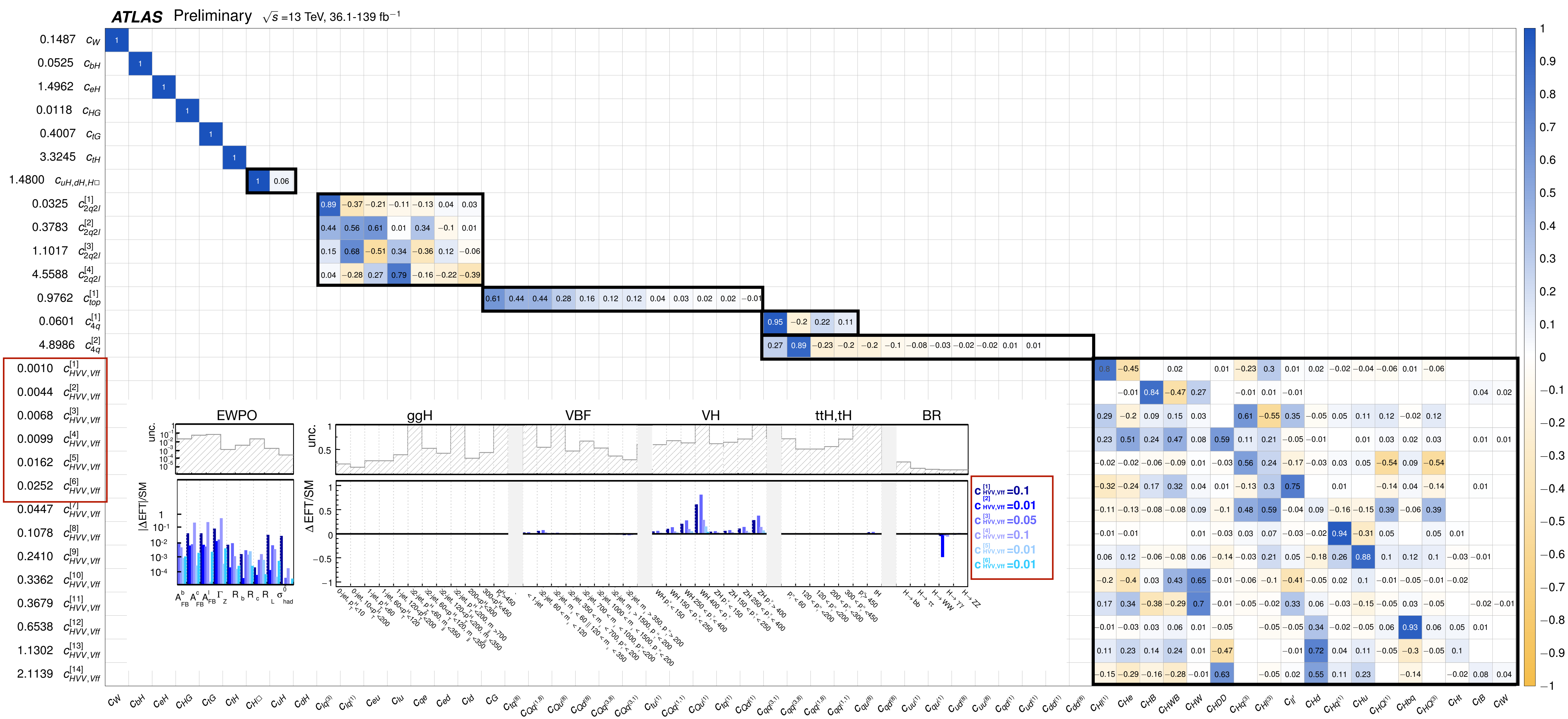

Warsaw Basis, Wilson coefficients